Supplemental Materials

Modulating inflammatory monocytes with a unique microRNA gene signature ameliorates murine ALS

Oleg Butovsky[1], Shafiuddin Siddiqui[1], Galina Gabriely[1], Amanda J. Lanser[1], Ben Dake[1], Gopal Murugaiyan[1], Camille E. Doykan[1], Pauline M. Wu[1], Reddy R. Gali[2], Lakshmanan K. Iyer[3], Robert Lawson[4], James Berry[4], Anna M. Krichevsky[1], Merit E. Cudkowicz[4] and Howard L. Weiner[1]

[1]Department of Neurology, Center for Neurologic Diseases, Brigham and Women's Hospital, Harvard Medical School; [2]The Harvard Clinical and Translational Science Center, Harvard Medical School; [3]Department of Neuroscience, Tufts School of Medicine; [4]Department of Neurology Massachusetts General Hospital, Neurology Clinical Trial Unit, Harvard Medical School, Boston, MA 02115.

Supplemental Methods

Behavioral Analysis. ALS mice were analyzed at day 30 and 60 (presymptomatic), day 90-100 (early symptomatic), and day 120-140 (late symptomatic/end-stage) time points. Onset of symptoms was defined by the peak of the weight curve and visible signs of muscle weakness. End-stage disease was determined by symptomatic progression and animal care guidelines (thus it varied from the 135 time-point by ±5 days). Disease progression was documented according to established methodology provided by Prize4Life and The Jackson Laboratory (1). Symptomatic analysis was conducted by daily monitoring and weight measurements every 3-4 days starting at day 80. Symptomatic onset was defined as the age at which animals began to decline in weight (2). In Figure 12E, the early symptomatic phase was defined as the time between disease onset (peak weight) to a 5% drop in weight; late symptomatic phase was defined as the time between a 5% drop in weight and end-stage. Neurological scores for both hind legs were assessed daily for each mouse beginning at 50 days of age. The neurological score used a scale of 0 to 4 developed by ALSTDI (3). Criteria used to assign each score level were: 0 = Full extension of hind legs away from the lateral midline when the mouse is suspended by its tail, and mouse can hold this position for 2 seconds, suspended 2–3 times; 1 = Collapse or partial collapse of leg extension towards lateral midline (weakness) or trembling of hind legs during tail suspension; 2 = Curling of the toes and dragging of at least one limb during walking; 3 = Rigid paralysis or minimal joint movement, foot not being used for forward motion; 4 = Mouse cannot right itself within 30 seconds from either side, euthanasia.

Generation of chimeric mice. Recipient lethally irradiated (950 Rad) 60 day old B6/SJL-SOD1^{G93A} and B6/SJL-WT mice were transplanted with donor syngeneic BM cells from CX3CR1-GFP$^{+/-}$-WT mice. Donor F1 B6/SJL-CX$_3$CR1-GFP$^{+/-}$ mice were generated by crossing homozygous B6-CX3CR1-GFP$^{+/+}$ to SJL-WT mice. In these chimeras, peripheral monocytes are distinguishable from microglia by FACS. Since CX3CR1 is expressed on myeloid cells, all peripheral BM-derived macrophages express GFP (4). Since radiation-resistant microglia have very slow turnover in adult CNS (5), all CNS-derived CD11b^{+}/CD39^{+} microglia were GFP-negative. We determined the percentage of chimerism 8 weeks after transplant by examining cells from the spleen. We found that 95–97% of F4/80^{+}CD11b^{+} cells in the spleen were GFP^{+}. In chimeric SOD1 mice, mononuclear cells stained for the monocyte marker CD11b could be easily subdivided into three distinct subsets: 1) CD11b^{+}/GFP^{-}/CD39^{+} microglia; 2) CD11b^{+}/GFP^{+}/CD39^{-} peripheral macrophages; 3) CD11b^{-}/GFP^{-} lymphocytes (Figure 10E).

Generation of monoclonal antibodies specific for resident microglia and peripheral inflammatory monocytes. Adult Lewis rat was vaccinated (ip) five times (two weeks apart) with adult freshly isolated microglia cells (5-10x10^{6} per vaccination) sorted with CD45-PerCp and CD11b-PeCy7 antibodies (BD Biosciences) from brains and spinal cords of C57/Bl6J (8-10 weeks old) mice. The first vaccination was performed with Complete Freund's Adjuvant and then next 3 injections with Incomplete Freund's Adjuvant with live microglia. The final boost was with cells injected both i.v. and i.p. to generate rat hybridoma cells producing specific microglia antibodies. Hybridoma positive oligoclones for microglia or peripheral monocytes were screened and identified by FACS for microglia positive/BM-monocytes negative antibody using pooled murine CD11b^{+}/CD45^{Low} adult microglia isolated from C57/Bl6J mice and GFP^{+} bone marrow (BM)-derived monocytes isolated from CX3CR1-GFP mice (Supplemental Figure 1A). 3-5 additional subclonnings were performed to produce 4D4, 5E12 and 6C3 monoclonal antibodies (mAbs). Hybridoma cells producing CD39 (5E12) and Ly6C (6C3) mAb were grown in bioreactor (Integra) to produce sufficient amount of antibodies for systemic injections in SOD1 mice. Endotoxin was removed below 0.1U using Detoxi-Gel Endotoxin Removing Gel kit (Thermo Scientific).

Cell transfection. For expression of Ly6C and CD39 in vitro, CHO-K1 cells (ATCC) were transfected with Myc-DDK-tagged ORF clone of mouse lymphocyte antigen 6 complex, locus C1 and C2 (Ly6C1, Ly6C2) and mouse ectonucleoside triphosphate diphosphohydrolase 1 (*Entpd1*; CD39). All transfection vectors were purchased from OriGene. Lipofectamine2000 (Invitrogen) was used to transfect CHO-KI cells with the plasmids.

Flow Cytometry. Mononuclear cells were directly isolated from the CNS of mice as described (6) except that no dispase was used as we found that dispase shades off several surface molecules and may diminish their surface detection. Mice were transcardially perfused with ice cold phosphate-buffer saline (PBS), spinal cords and brains separately dissected. Single cell suspensions were prepared and centrifuged over a 37%/70% discontinuous Percoll gradient (GE Healthcare), mononuclear cells isolated from the interface, and total cell count determined. Cells were pre-blocked with anti-CD16/CD32 (Fc Block BD Biosciences), and stained on ice for 30 min with combinations of anti-CD45-FITC, anti-Ly6C-FITC, CD11b-PE-Cy™7, rat IgG isotype controls (from BD Biosciences). 5E12 (CD39) and 6C3 (Ly6C) mAbs were directly conjugated to or Alexa Fluor® 488 or 647 (Invitrogen) or detected with goat anti-rat IgG conjugated to FITC (Biolegend). PE or FITC-conjugated-CD169 was detected by FACS as described previously (7). Combination of AnnexinV-PE or -FITC-conjugated and 7AAD-PerCP was used to stain apoptotic and necrotic cells, respectively (BD Biosciences). APC- or FITC-conjugated anti-BrdU antibodies were used to detect microglia and monocyte proliferation (BrdU Flow Kit; BD Biosciences). Appropriate antibody IgG isotype controls (BD Biosciences) were used for all stains. We used 5E12 and 6C3 mAbs in all experiments except for CD39 (eBisoscience) and Ly6C mAbs (BD Biosciences) for validation experiments showed in Supplemental Figure 2. Fluorescence-activated cell sorter (FACS) analysis was performed on a LSR machine (BD Biosciences), and data subsequently analyzed with FlowJo Software (TreeStar Software).

Patients. Blood and cerebrospinal fluid (CSF) collection was carried out via convenience sampling of patients recruited from the Massachusetts General Hospital (MGH) Muscular Dystrophy Association ALS clinic and the MGH Neurology Clinical Trials Unit. Blood samples from untreated relapsing-remitting multiple sclerosis patients were collected at the Partners Multiple Sclerosis Center, Brigham and Women's Hospital (BWH) and matched healthy control volunteers were collected at the Center for Neurologic Diseases, (BWH). Patients receiving an experimental therapy within the month prior to blood collection or with unstable medical conditions outside of ALS were excluded. Study volunteers donating blood were enrolled over the period from 01/04/2011 to 09/06/2011; those donating CSF were enrolled over the period from 02/09/1998 to 12/14/2010 The ALSFRS-R (revised ALS Functional Rating Scale) is a previously validated 48-point scale reflecting ALS disease severity (8-10). Disease severity of MS patients was in the range of 2.5-3.5 on the EDSS (expanded disability status scale) (11).

Blood samples. Blood samples were collected from 24 healthy control donors, 22 patients with sporadic ALS (sALS), 4 patients with familial ALS (fALS) due to mutations in the SOD1 gene, and 8 relapsing-remitting MS patients. All four fALS patients carried the SOD1 mutation, with specific mutations, including A10G, L113T, A4V, and L9V (Supplemental Table 7). Blood was drawn by a study phlebotomist using standard equipment and collected in lithium heparin tubes. Samples were transported to the lab for cell separation within 4 hours of collection. Cells were then frozen until use.

Cerebrospinal fluid (CSF) samples. CSF samples were collected from 10 patients with sALS, 5 with fALS, and 10 volunteers without a history of neurologic disease or relatives with ALS (Supplemental Table 8). 10 Parkinson's disease (PD) donors were obtained from Harvard NeuroDiscovery Center and Neurology Clinical Trial Unit Harvard Medical School, Boston. All human materials were obtained and used in accordance with the policies of institutional review board at Brigham and Women's and Massachusetts General Hospital. CSF was obtained via lumbar puncture performed by an experienced neurologist and collected into polystyrene tubes prior to processing. At least one ml of each CSF sample was cleared of cells and debris immediately after collection by brief centrifugation and stored in aliquots at -80°C.

Isolation of human blood monocytes. Fresh peripheral blood mononuclear cells were obtained by Ficoll density-gradient centrifugation. $CD14^+/CD16^-$ and $CD14^+/CD16^+$ monocyte subsets stained with mouse anti-human CD14-PE and CD16-PeCy7 (BD Pharmingen) were sorted with a FACSAria (BD Biosciences). The sorted cells were further prepared for the RNA isolation protocol indicated below.

Analysis of miRNA and mRNA expression. To assess microRNA and mRNA expression in human $CD14^+/CD16^-$ and $CD14^+/CD16^+$ monocyte subsets and brain and spinal cord CD11b+/CD39 microglia and CD11b/Ly6C spinal cord and splenic monocytes from WT and SOD1 mice, total RNA was isolated and

analyzed by qRT-PCR using specific primers for selected mRNAs and miRNAs all purchased from Applied Biosystems. For analysis of miRNA expression, qRT-PCR analyses were carried out using TaqMan miRNA assays (Applied Biosystems) and relative expression was calculated using the ΔC_T method as described elsewhere (12) and normalized to uniformly expressed U6 (Applied Biosystems) for miRNAs and house-keeping genes for relative gene expression indicated in each corresponding figure legends. All qRT-PCRs were performed in duplicate or triplicate, and the data are presented as mean ± standard deviations (SD).

Administration of BrdU and tissue preparation. The cell-proliferation marker BrdU was dissolved by sonication in PBS and injected i.p. (50 mg/kg body weight) daily for 5 days starting on day 85, 115 and 130 of age in $SOD1^{G93A}$ and WT-littermates. 12 hours after the last BrdU injection, the animals were deeply anesthetized and perfused transcardially, first with PBS and then with 2.5% paraformaldehyde. Their spinal cords were removed, postfixed overnight, and then equilibrated in phosphate-buffered 30% sucrose. Free-floating 30-µm axial sections were collected on a freezing microtome (SM2000R; Leica Microsystems) and stored at 4°C prior to immunohistochemistry.

Immunohistochemistry. Transverse sections of the spinal cord or coronal sections of the brain (30 µm) were treated with a permeabilization/blocking solution containing 10% FCS, 2% bovine serum albumin, 1% glycine, and 0.05% Triton X-100 (Sigma-Aldrich). Primary antibodies were applied for 1 hour in a humidified chamber at room temperature. Sections were blocked for 1 hour with blocking solution. The tissue was then stained in combination with rat anti-4D4 mAb (1:2000; 4D4 clone), mouse anti-NeuN (1:500; Millipore) or rat anti-CD169 (1:200; Serotec), and rabbit anti-Iba1 (1:500; Wako) antibodies diluted in PBS containing 0.05% Triton X-100, 0.1% Tween 20, and 2% horse serum. Sections were incubated with the primary antibody for 12 hours at 4°C, washed with PBS, and incubated with the secondary antibodies in PBS for 1 hour at room temperature while protected from light. Secondary antibodies used for both immunocytochemistry and immunohistochemistry were donkey anti-rat or donkey anti-sheep Cy3, donkey anti-rabbit Cy5; donkey anti-mouse FITC. All antibodies were purchased from Jackson ImmunoResearch Laboratories Inc. and used at a dilution of 1:250–1:500. Control sections (not treated with primary antibody) were used to distinguish specific staining from staining of nonspecific antibodies or autofluorescent components. Sections were then washed with PBS and coverslipped in polyvinyl alcohol with diazabicylo-octane anti-fading agent or ProLong® Gold antifade reagent with DAPI (Invitrogen).

RNA isolation and miRNA profiling in CSF. CSF samples were lyophilized and total RNA was extracted using mirVana miRNA isolation kit (Ambion) according to the manufacturer's protocol. The amount of RNA extracted from the CSF samples was in the 50-2500 ng/ml range, consistent with the previous findings (13). The levels of individual miRNAs in CSF were determined by TaqMan miRNA assays from Applied Biosystems. 2-4 ng of total RNA was used in 6 µl of reverse transcription reaction with specific miRNA RT probes, prior to TaqMan real-time PCR reactions that were performed in duplicates. miR-125b, which is abundantly expressed in brain (14), was detected in CSF samples and used as an internal control for normalization. miRNAs levels were calculated relative to corresponding miR-125b levels by the formula 2^(-ΔCt), where $\Delta Ct = Ct_{miR\text{-}X} - Ct_{miR\text{-}125b}$. All data are mean of duplicates, and the standard errors of mean were calculated between duplicates.

Taqman® microRNA Low density arrays (TLDA) miRNA analysis. The ABI Taqman® microRNA Low density arrays (TLDA, Applied Biosystems, Foster City, CA, http://www.appliedbiosystems.com) were selected as the platform for microRNA profiling in WT and SOD1 mice. This platform consists of 2 arrays: TLDA panel A (377 functionally defined microRNAs) and TLDA panel B (289 microRNAs whose function is not yet completely defined). Each array/panel includes, among other endogenous controls, the mammalian U6 (MammU6) assay that is repeated four times on each card as a positive control. This platform represented comprehensive Taqman Low Density Array (TLDA) for global screening of miRs for which commercially available primer-probe sets existed that were extensively validated. Total RNA was isolated using mirVana miRNA isolation kit (Ambion) from sorted $CD11b^+/CD39^+$ spinal cord microglia and splenic $CD11b+/Ly6C^{Hi}$ monocytes from WT and SOD1 mice at presymtomatic (60d), onset and end-stage (*n*=6-8 mice per group). RNA quality was assessed using Nanodrop (OD 260/280 and 260/230) and bioanalyzer provided by the Biopolymers Facility at Harvard Medical School. The overall microRNA profiling of these groups included a total of 16 Taqman ® microRNA Low density arrays (TLDAs). For each biological specimen, two TLDA panel A were run. RNA

reverse transcription was accomplished according to the ABI microRNA TLDA Reverse Transcription Reaction protocol.

TLDA Data Analysis. TLDA were run in the 7900 HT Sequence Detection system. The ABI TaqMan SDS v2.3 software was utilized to obtain raw CT values. To review results, the raw CT data (SDS file format) were exported from the Plate Centric View into the ABI TaqMan RQ manager software. Automatic baseline and manual CT were set to 0.2 for all samples.

Statistical analysis of TLDA data. TLDA data was normalized using quantile (R software) to remove variation between samples. miRNA profiling of splenic Ly6C^{Hi} monocytes and spinal cord-derived microglia were analyzed using bioconductor one channel GUI package to calculate the expression. To find significantly affected miRNAs in splenic Ly6C^{Hi} monocytes and spinal cord-derived CD39+ microglia in SOD1 mice compared to non-Tg mice the raw data was subjected to quantile normalization algorithm using bioconductor's HTqPCR to produce a uniform empirical distribution of Ct values followed by linear models fit program of Limma package. Significant differential expression with $P < 0.05$ miRNA were generated. Next, input data for class comparison, permutations and prediction analysis consisted of the miR expression CT values was normalized to the endogenous housekeeping MammU6 (CT, sample - CT, MammU6). miRNA expression between WT and SOD1 mice was compared by ANOVA with Dunnett's post-hoc test.

Quantitative NanoString nCounter miRNA/gene expression analysis. Nanostring nCounter technology (nanostring.com) allows expression analysis of multiple genes (up to 800 genes) from a single sample. It does not require the conversion of mRNA to cDNA by reverse transcription or the amplification of the resulting cDNA by PCR (15). Furthermore, it allows expression analysis of rare cells (at most 3,000-10,000 cells) which is perfectly suited for the limited number of cells infiltrating the CNS. Nanostring nCounter gene expression is more sensitive than microarrays, is similar in accuracy to qRT-PCR, and more scalable than qRT-PCR or microarrays in terms of time, effort and sample requirements (16-18). We performed multiplexed target profiling of 179 inflammation- and 511 immune-related transcripts which consist of genes differentially expressed during inflammation and immune responses and 664 human miRNAs (see complete list of genes and miRNAs at nanostring.com). This combination of genes and miRNAs and their differential expression in CD39^{+} microglia and Ly6C^{+} monocyte subsets allowed us to interrogate immune-related pathways using the GeneGo and Ingenuity® pathway analysis during disease progression in ALS mice.

GeneGo Biological Pathway Analysis. We compared differentially regulated genes in spinal cord CD39+ microglia and splenic Ly6C^{Hi} monocytes in SOD1 mice and blood-derived CD14^{+}/CD16^{-} monocytes from HC vs. sALS subjects using GeneGO Metacore pathway analysis (GeneGO, St. Joseph, MI; genego.com). This method identified transcripts that are overrepresented in defined ontologies. A false discovery rate (FDR) filter was applied to preliminary P values, using a q-value calculation. After the enrichment, P values are calculated for all the terms within the given ontology, each term is tested as a separate hypothesis, and the resulting q-values represent corrected P values with account of total terms in the given ontology and the rank order of the particular term. The identified significantly affected genes were further analyzed to identify biological/disease processes and the involved pathways/networks in SOD1 mice and human ALS. The whole data set of 58 affected genes in CD39^{+} microglia from spinal cord and 47 affected genes in Ly6C^{Hi} splenic monocytes in SOD1 mice were imported into MetaCore to build an analysis of functional ontologies including GeneGo process, GeneGo disease process, canonical pathway maps, and networks. Calculation of statistical significance throughout MetaCore for maps, networks, and processes are based on P values, which are calculated based on hypergeometric distribution. P values essentially represent the probability of particular mapping arising by chance given the numbers of genes in the set of all genes on maps/networks/processes, genes on a particular map/network/process, and genes in the experiment (19). We used a P value of 0.01 for the cutoff. The degree of relevance to different categories for the uploaded data sets is defined by P values, so that the lower P value obtains higher priority. The experimental data were input to build networks. The three different scoring functions used to rank the small subnetworks created by the network building algorithms were zScore, gScore, and p value. The zScore ranks the subnetworks (within the analyzed network) with regards to their saturation with genes from the experiment. A high zScore means the network is highly saturated with identified affected genes from the experiment. In other words, it means that relatively larger number of

genes/analytes in a particular network were present in the aqueous sample. Each network is comprised of canonical pathways. The gScore modifies the zScore based on the number of canonical pathways used to build the network. If a network has a high gScore, it is saturated with expressed genes (from the zScore), and it contains many canonical pathways. We controlled for multiple testing by estimating the false discovery rate. Out of 664 microRNAs measured, 56 were confidently detected; 20 were differentially expressed in at least one disease group.

IPA (Ingenuity®) miRNA-mRNA target filter analysis. To investigate the statistical significance of the miRNA-mRNA interaction, we used the Targetscan 4.1 prediction of 862044 conserved miRNA binding sites with non-zero context score which is a measure of conservation. In the SOD1 mouse dataset: miRNA target filtering analysis using IPA results in 34 miRNA families that are predict to target 10797 mRNAs. To focus our studies to genes involved in immune response, we filtered these predicted miRNA-mRNA interactions to include only those genes involved in the IPA Canonical Pathway categories representing signaling pathways involved in Cellular Immune Response, Humoral Immune Response and Cytokine Signaling. This resulted in filtering of the 34 microRNAs to target 971 mRNAs possibly involved in immune response signaling. To further focus our analysis, we integrated the mRNA expression studies using the Nanonstring platform into this analysis. We filtered the 971 targets to contain the 47 immune related genes that are affected in SOD1 mice taking into account the opposite nature of the miRNA-mRNA regulation. This resulted in a final 87 pairs of miRNA- mRNA interactions representing, 27 miRNA families and 33 mRNAs. In our miRNA expression of ALS subjects study, 56 miRNAs were found to be significantly affected in ALS subjects. Filtering the predicted 862044 to those containing only targets of these 56 miRNAs resulted in their reduction to 34118 sites. Further, if we restrict the mRNA targets to be on genes found to be regulated with a fold change of >1.4 in our Immunological Panel Nanostring arrays, we generated a final 68 unique miRNA-mRNA interaction pairs for our dataset in which the mRNA and miRNA are oppositely regulated. The statistical significance of these 68 miRNA-mRNA interactions formed by 56 affected miRNAs were assessed as follows: 1) we generated 1000 random networks in which 56 randomly selected, non-regulated miRNAs from our study were used to find mRNAs which contained a 3'UTR motif for their binding. 2) These miRNA-mRNA pairs were further filtered to contain only those 59 mRNAs that were affected in ALS subjects. It shows a mean of 44.88 interactions (SD = 9.99). The true interactions determined in out expression studies is 68 and corresponds to significant P-value < 1.1E-15. A similar analysis for the regulated miRNA-mRNA pairs in the SOD1 mice shows an interaction distribution with a mean of 15.26 (SD = 4.03) whereas the true miRNA-mRNA interactions determined experimentally is 41 with significant P-value of < 5.7E-9. The distribution of these random miRNA-mRNA interactions is shown in Supplemental Figure 13. This analysis shows that the putative miRNA-mRNA interactions that we observe in both the ALS subject and SOD1 mice are statistically significant. IPA provides the most comprehensive, validated knowledgebase of interactions between biomolecules including miRNA. Further, they also provide comprehensive annotation of different functional and pathway enrichment along with the ability to present this knowledge in the form of a network of interaction. In our case, we are interested in the miRNA-mRNA interactions focusing on those that are specifically involved in immune response signaling. With this in mind, we further analyzed our miRNA and mRNA expression dataset using IPA.

Supplemental Figures

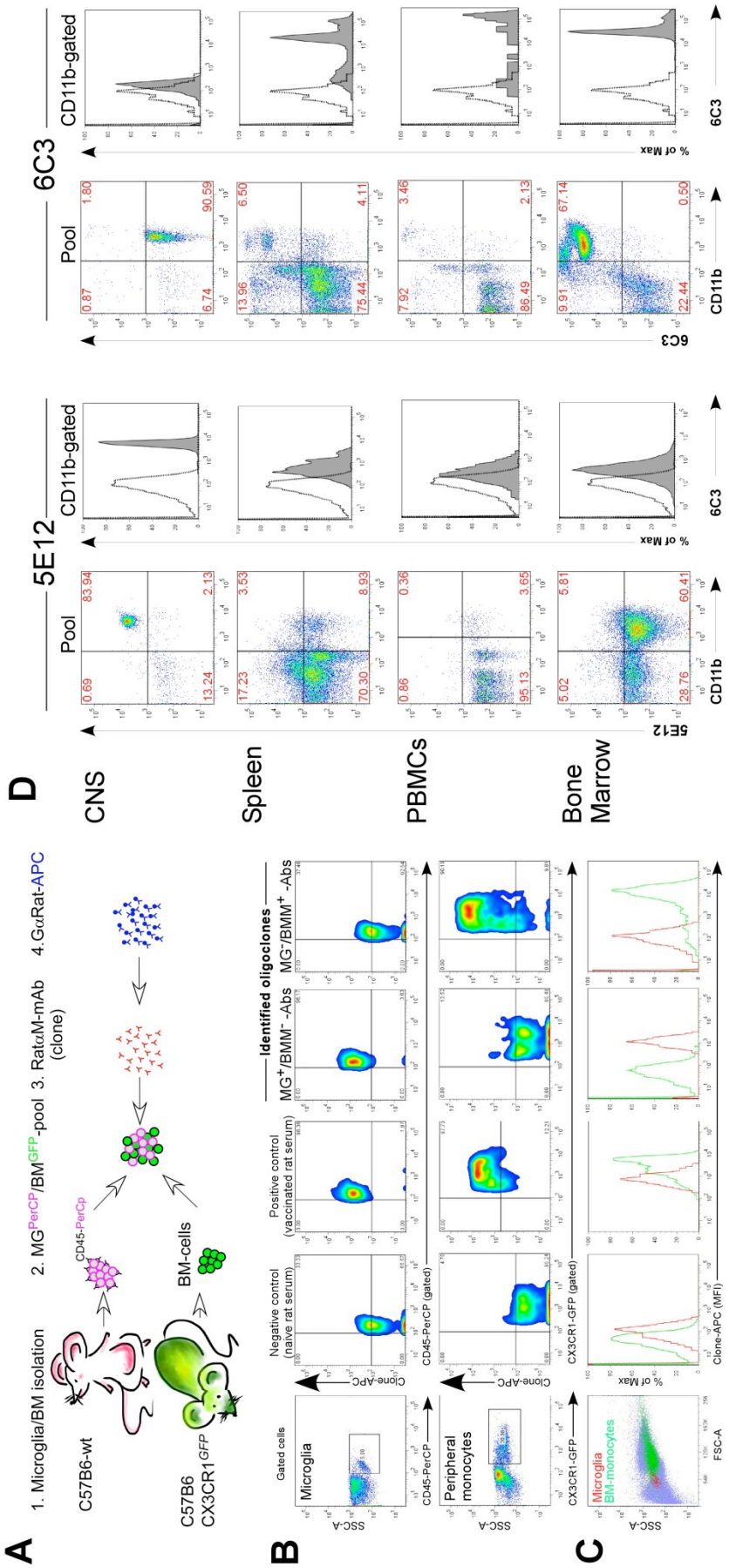

Supplemental Figure 1. Generation of monoclonal antibodies that identify resident microglia and peripheral monocytes. (A) Schematic diagram of high throughout screen (HTS) designed to identify unique hybridoma antibodies against peripheral bone marrow (BM)-derived monocytes and adult microglia cells. A Lewis rat was immunized with microglial cells and oligoclonal antibodies were obtained as described in Supplemental methods. BM-derived monocytes from $CX3CR1^{GFP/+}$ transgenic mice, expressing GFP in all mononuclear cells(4), were isolated and pooled with WT-adult microglia cells extracted by Percoll and pre-stained with CD45-PerCP. Pooled cells were screened against the rat anti-mouse oligoclonal antibodies and detected with secondary goat anti-rat APC-conjugated antibodies. Hybridoma cells were selected by FACS for microglia and BM-monocytes antibodies. Out of 12,000 hybridoma oligoclones, 16 hits were identified (70% microglia+ and 30% both or BM+), with 2 antibodies: 5E12 and 6C3, respectively specific for microglia and BM-derived monocytes. **(B)** FACS histograms represent an example of identified oligoclones positive for microglia or BM-derived monocytes. Gated microglia ($CD45^{+}$) and BM-derived monocytes (GFP^{+}) were further analyzed and identified oligoclones were subcloned three to five times to generate monoclonal specific antibodies (mAb) to microglia and peripheral monocytes. Identified oligoclones were rescreened with HTS LSR instrument to generate hybridoma monoclones. **(C)** Flow cytometry histograms show mean fluorescence intensity (MFI) of surface expression of microglial specific 5E12 (red line) and BM-derived monocytes specific 6C3 (green line) oligoclonal antibodies. **(D)** Specificity of 5E12 and 6C3 mAb for CNS-derived microglia and peripheral BM-derived monocytes. FACS analysis of pooled cells or CD11b-gated mononuclear cells derived from naive adult mouse CNS and peripheral organs including spleen, PBMCs and bone marrow (BM) stained for identified microglial (5E12) and peripheral monocytes specific (6C3) mAbs. Filled histograms show 5E12 and 6C3 staining; open histograms show staining for isotype control.

Supplemental Figure 2. Identification of Ly6C and CD39 molecules recognized by 6C3 and 5E12 mAb.

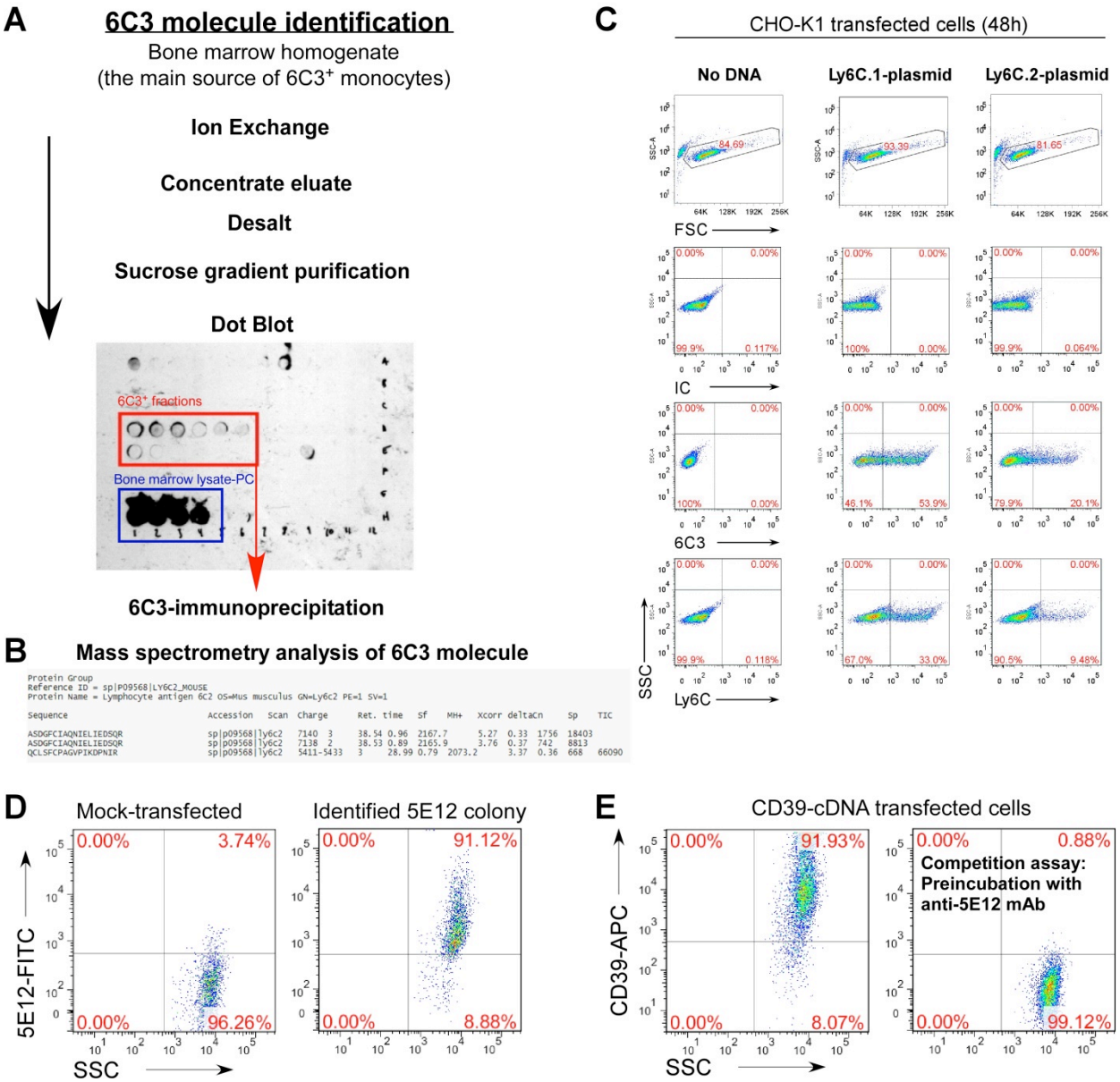

Supplemental Figure 2. Identification of Ly6C and CD39 molecules recognized by 6C3 and 5E12 mAb. (A) Bone marrow-derived monocytes were used as the main source for 6C3 antigen expressed by $CD11b^+$ cells. 6C3 antigen purification was performed by ion exchange chromatography following linear sucrose gradient fractionation. $6C3^+$ positive fractions detected in dot blot (red boxed area) were pooled and the 6C3 molecule further purified by immunoprecipitation with anti-6C3 mAb. Note, whole bone marrow protein lysate was used as a positive control (blue box, serial dilutions). **(B)** Mass spectrometry analysis identified the Ly6C.2 isoform as the molecule recognized by 6C3 mAb. **(C)** FACS analysis of CHO-K1 cells 48h post-transfection with cDNA expression vectors of Ly6C.1 and Ly6C.2 isoforms. No $Ly6C^+$ signal was detected in mock-transfected (no plasmid DNA) cells or CHO-K1-transfected cells detected with isotype control (IC). Both 6C3 and commercial Ly6C antibodies identify both Ly6C.1 and Ly6C.2 isoforms in CHO-K1-transfected cells with Ly6C expression plasmids. **(D)** 293T cells were transfected with normalized microglial cDNA library generated from $CD11b^+/5E12^+$ sorted adult microglia cells. 5E12 mAb recognized microglial cDNA-293T-transfected cells with a microglial cDNA clone. Gene sequence analysis of the $5E12^+$ cDNA colony identified CD39 gene. **(E)** Both 5E12 and commercial CD39 APC-conjugated mAb immunoreactive to 293T cells transfected with CD39-cDNA expression plasmid 48h after transfection. Note, pre-incubation of CD39-transfected 293T cells with 5E12 mAb completely abrogated detection of CD39 molecule with commercial CD39 antibody.

Supplementary Table 1. Significantly affected genes in CD39+ spinal cord microglia in SOD1 mice

Affected genes	Fold change vs. Non-Tg			P value vs. Non-Tg		
Upregulated Genes	**Presympt (60d)**	**Onset**	**End-Stage**	**Presympt (60d)**	**Onset**	**End-Stage**
Ccl2	5.5	12.1	28.2	4.0E-04	7.7E-07	1.4E-03
Ccl4	6.3	15.1	16.5	6.8E-04	1.8E-04	3.2E-04
Csf1	4.2	8.5	13.1	8.9E-03	1.8E-04	8.6E-04
Cxcr4	2.7	7.7	11.8	2.6E-01	5.7E-04	2.5E-04
Ccl3	5.1	10.4	5.3	1.7E-01	3.4E-03	7.9E-04
Il1b	4.0	9.2	7.0	3.4E-03	4.2E-04	6.8E-04
Maff	3.0	7.1	7.6	2.5E-02	6.5E-04	2.7E-04
Cxcl10	3.5	3.7	8.3	6.9E-03	1.0E-03	2.0E-04
C4a	3.9	3.5	5.9	3.7E-03	7.2E-04	2.0E-03
Ccl5	3.0	4.7	5.3	6.8E-03	2.7E-03	1.6E-03
C3	2.0	3.5	4.5	4.9E-01	3.7E-01	1.0E-03
Il18rap	1.1	1.7	5.9	8.6E-01	2.3E-02	5.0E-03
Tlr2	1.7	2.7	4.3	6.9E-02	4.4E-03	7.1E-03
Tnf	1.8	2.9	3.3	6.6E-01	3.5E-02	5.3E-03
Pdgfa	1.6	2.8	3.3	9.9E-02	1.3E-02	2.1E-03
C3ar1	1.5	2.0	3.4	1.9E-01	7.1E-03	1.2E-03
Bcl6	1.2	2.2	3.4	1.2E-01	2.8E-03	1.2E-03
Pgk1	1.7	1.8	2.0	1.6E-01	1.1E-02	6.4E-03
Gnas	1.4	1.6	2.2	7.8E-02	5.5E-02	1.1E-02
Il1r1	1.1	1.3	2.0	1.8E-01	1.3E-01	9.7E-03
Downregulated Genes	**Presympt (60d)**	**Onset**	**End-Stage**	**Presympt (60d)**	**Onset**	**End-Stage**
Tlr5	-1.8	-6.7	-11.8	1.6E-02	2.0E-03	9.8E-04
Il6	-1.7	-4.2	-8.2	1.2E-02	2.8E-03	8.9E-04
Ccl24	-2.1	-4.1	-6.8	2.2E-02	1.4E-02	1.3E-02
Myl2	-1.6	-3.0	-7.4	3.6E-03	5.2E-04	3.0E-04
Prkca	-1.6	-3.1	-4.5	4.1E-03	3.1E-04	2.4E-04
Ccr1	-2.3	-2.0	-4.1	3.7E-03	4.5E-03	2.3E-03
Il6ra	-1.4	-3.0	-3.1	1.2E-03	1.1E-04	1.9E-05
Tlr3	-1.4	-2.0	-3.1	6.6E-03	6.2E-04	3.8E-05
Rps6ka5	-1.2	-2.4	-2.9	1.2E-01	1.3E-03	1.8E-04
Mef2a	-1.5	-2.5	-2.5	3.9E-02	6.9E-03	3.0E-03
Il18	-1.4	-2.5	-2.6	5.9E-03	2.3E-03	6.0E-04
Nr3c1	-1.4	-2.5	-2.5	1.2E-02	5.6E-04	1.3E-03
Pla2g4a	-1.2	-3.1	-2.0	7.9E-02	3.5E-03	6.2E-03
Myd88	-1.4	-2.3	-2.4	2.2E-02	1.3E-03	1.5E-03
Map3k5	-1.5	-1.9	-2.6	4.9E-03	5.1E-04	4.9E-04
Map2k1	-1.4	-2.0	-2.5	4.5E-02	4.8E-03	1.4E-03
Jun	-1.9	-2.5	-1.5	2.3E-03	3.7E-03	4.2E-02
Map2k6	-1.1	-2.0	-2.7	6.6E-02	5.1E-03	9.8E-04
Rock2	-1.2	-2.1	-2.6	6.2E-03	4.1E-04	2.9E-04
Mapk14	-1.2	-2.0	-2.5	1.0E-02	1.3E-03	1.2E-03
Creb1	-1.1	-2.0	-2.5	6.1E-02	9.8E-03	6.0E-03
Il15	-1.2	-2.0	-2.4	1.1E-01	1.6E-02	3.6E-02
Mef2c	-1.1	-1.9	-2.5	6.6E-02	1.5E-03	2.9E-03
Rapgef2	-1.6	-2.0	-1.9	3.1E-02	3.6E-03	4.2E-03
Rac1	-1.3	-2.3	-1.9	3.0E-02	2.2E-03	7.9E-03
Fos	-1.5	-1.6	-2.4	2.1E-03	2.2E-03	1.1E-03
Mapk8	-1.4	-2.2	-1.7	4.9E-03	4.5E-04	6.1E-04
Max	-1.5	-1.5	-2.5	4.0E-02	6.7E-03	2.9E-03
Tlr6	-1.3	-1.7	-2.5	9.5E-03	5.6E-03	6.3E-04
Rhoa	-1.4	-1.9	-2.0	1.3E-02	1.3E-04	5.4E-04
Ripk2	-1.2	-1.9	-2.2	2.5E-02	9.5E-04	5.9E-04
Tlr4	-1.5	-2.0	-1.8	4.1E-03	6.2E-04	2.1E-04
Mknk1	-1.4	-1.8	-1.9	1.8E-02	9.2E-04	2.9E-04
Tgfb1	-1.3	-1.9	-2.0	2.3E-02	2.0E-04	1.3E-03
Tgfbr1	-1.4	-1.9	-1.7	1.3E-02	2.7E-04	1.6E-03
Map3k1	-1.3	-1.8	-1.7	6.3E-02	1.6E-02	9.0E-02
Il1a	-1.3	-1.3	-1.7	1.8E-01	1.5E-02	2.6E-03
Mef2d	-1.3	-1.6	-1.4	3.8E-02	1.9E-04	2.2E-02

Supplemental Table 1. **Significantly affected genes in CD39+ spinal cord microglia in SOD1 mice.** Note, values represent fold change of significantly up or downregulated genes in SOD1 mice from non-Tg littermates at each time-point. Data represents mean of three independent experiments (pooled from 4-5 mice in each experiment; see Figure 2 A and B). *P* values represent statistical differences between 2 groups by Student's t test (2-tailed).

Supplementary Table 2. Significantly affected genes in Ly6C^{Hi} splenic monocytes in SOD1 mice

Affected genes	Fold change vs. Non-Tg			P value vs. Non-Tg		
Upregulated Genes	**Presympt (60d)**	**Onset**	**End-Stage**	**Presympt (60d)**	**Onset**	**End-Stage**
Tnf	5.4	6.4	4.8	2.1E-03	1.0E-03	1.2E-02
Ltb	3.7	4.5	7.9	2.1E-05	4.1E-05	5.8E-04
Tlr6	5.2	5.2	5.6	1.6E-04	2.2E-06	8.8E-05
Ccr2	5.9	6.3	3.7	2.6E-05	2.5E-05	2.3E-06
H2-Eb1	3.5	4.6	7.4	6.3E-08	4.9E-05	4.5E-05
Jun	7.5	3.4	3.1	2.1E-02	3.6E-03	5.7E-03
Rac1	6.1	4.3	1.8	6.4E-07	4.8E-07	4.6E-04
Hdac4	3.9	4.1	3.3	2.1E-02	1.6E-05	1.6E-03
Ccl5	4.0	4.0	3.0	1.3E-06	2.3E-03	5.0E-03
Atf2	4.8	3.2	3.0	2.7E-04	1.4E-05	1.3E-05
Tlr1	5.2	2.9	2.7	2.3E-03	3.2E-02	1.2E-03
Cd40	4.2	4.2	2.4	3.9E-04	2.7E-04	3.5E-04
Ripk2	3.5	3.4	3.8	1.8E-03	4.5E-04	4.8E-05
Myc	2.9	3.9	3.7	2.8E-04	7.2E-03	1.9E-02
Mapk1	3.5	3.2	3.5	1.3E-03	2.3E-05	5.6E-06
Rhoa	4.5	3.1	2.6	2.3E-05	4.9E-05	1.3E-05
Cfl1	4.2	3.5	2.4	8.1E-03	2.0E-03	1.4E-03
Daxx	3.9	3.7	2.4	7.5E-03	1.4E-03	2.1E-04
Il1b	3.5	3.9	2.4	5.8E-03	1.5E-04	4.9E-03
Stat1	3.4	3.8	2.6	1.9E-06	1.8E-03	1.0E-05
Mafk	4.3	3.3	2.0	3.9E-04	1.1E-03	4.5E-03
Cdc42	3.0	3.2	3.0	3.5E-05	5.5E-06	2.3E-04
Myd88	3.5	2.7	2.8	1.2E-06	2.7E-06	2.1E-04
Nr3c1	2.8	2.9	3.2	5.2E-05	5.4E-05	9.9E-05
Mapkapk2	3.3	2.9	2.7	7.0E-07	2.7E-06	1.3E-07
Mapkapk5	3.5	2.6	2.7	1.8E-04	1.8E-05	1.4E-04
Tlr2	3.6	2.9	2.2	2.1E-04	1.3E-04	8.2E-05
Fos	3.8	2.9	1.9	2.0E-06	3.8E-04	1.4E-04
Nfkb1	3.5	2.8	2.1	2.3E-03	1.6E-05	2.1E-06
Cxcr4	3.1	2.9	2.2	3.1E-05	6.8E-04	5.2E-06
Map2k1	3.2	2.9	1.9	2.3E-05	7.3E-06	3.1E-05
C3	3.2	2.9	1.9	1.5E-04	2.4E-03	2.9E-04
Map3k5	3.2	2.9	1.9	8.5E-05	1.1E-05	2.2E-03
Raf1	3.3	2.9	1.8	5.7E-06	3.6E-06	2.0E-03
Gnas	3.2	2.8	1.9	5.1E-07	4.7E-05	2.1E-05
Mapk14	3.2	2.8	1.9	2.1E-05	4.0E-07	3.1E-05
Tlr7	3.0	2.9	2.0	4.9E-06	1.7E-04	1.7E-06
Bcl6	2.7	2.8	2.4	5.0E-04	1.2E-04	6.0E-05
Il18rap	3.2	2.5	2.1	2.1E-04	9.7E-04	8.9E-03
Downregulated Genes	**Presympt (60d)**	**Onset**	**End-Stage**	**Presympt (60d)**	**Onset**	**End-Stage**
Cebpb	-2.8	-2.9	-2.2	9.5E-06	3.3E-05	3.3E-04
Tradd	-2.9	-2.7	-2.3	1.4E-04	3.6E-04	2.1E-03
Tgfbr1	-2.9	-3.2	-2.2	7.9E-06	6.5E-06	9.7E-05
Plcb1	-3.6	-2.8	-2.1	1.8E-05	2.5E-06	6.0E-04
Rapgef2	-4.5	-2.6	-2.2	2.1E-05	2.3E-04	3.3E-02
Mef2d	-3.7	-3.2	-2.8	7.7E-04	2.1E-04	1.1E-04
Tgfb1	-3.4	-4.0	-2.6	2.5E-04	5.7E-06	7.0E-07

Supplemental Table 2. **Significantly affected genes in Ly6C^{Hi} splenic monocytes in SOD1 mice.** Note, values represent fold change of significantly up or downregulated genes in SOD1 mice from non-Tg littermates at each time-point. Data represents mean of three independent experiments (pooled from 4-5 mice in each experiment; see Figure 3 A and B). *P* values represent statistical differences between 2 groups by Student's t test (2-tailed).

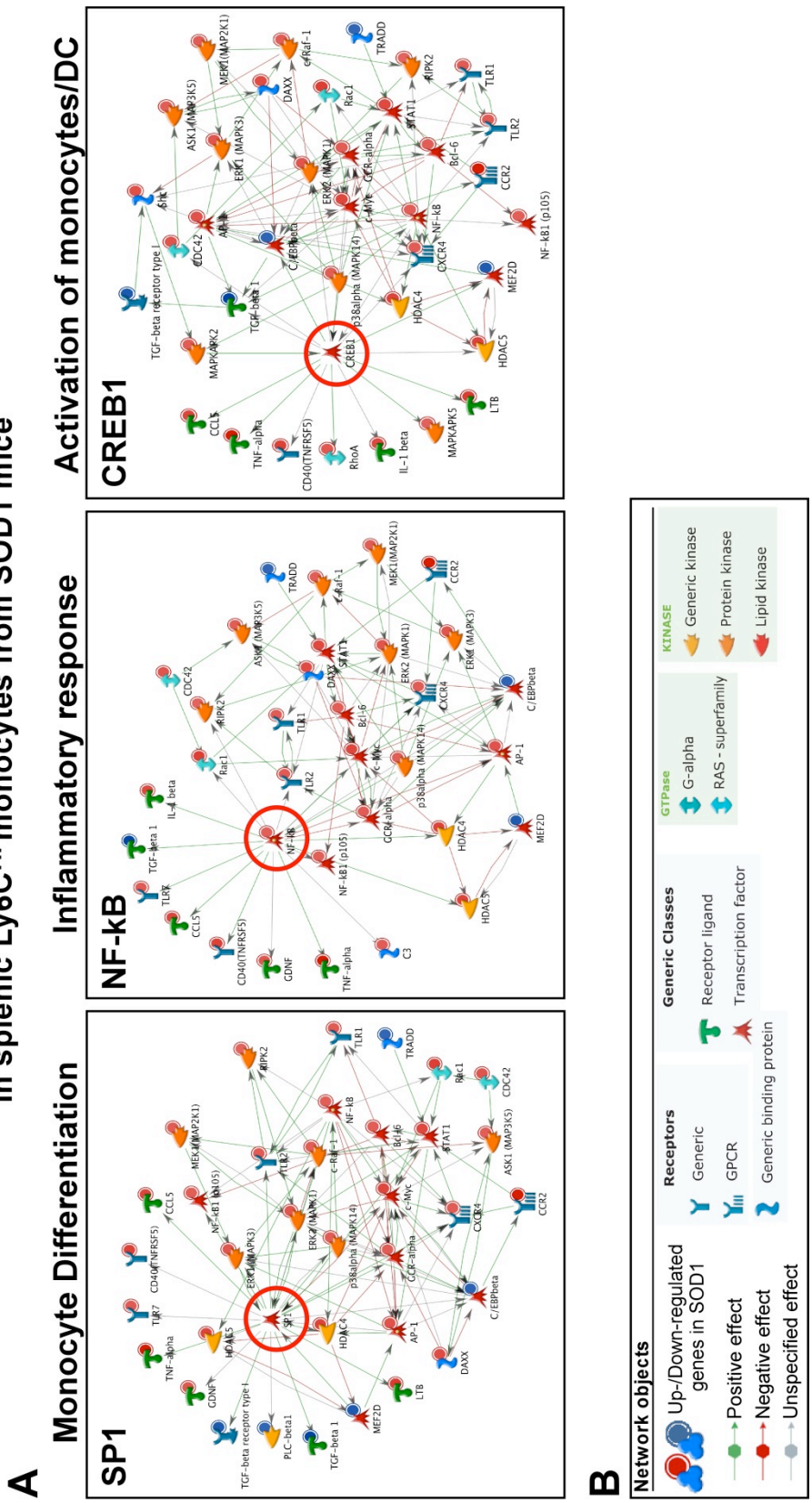

Supplemental Figure 3. Activation of pro-inflammatory pathways in splenic Ly6C^{Hi} monocytes from SOD1 mice. Biological network analysis based on differentially expressed inflammation-related genes in Ly6C^{Hi} monocytes at disease onset demonstrated significantly activated biological pathways (see Table 3). The most affected transcription factor networks related to monocyte activation were selected to demonstrate the genes involved in these networks. **(A)** Three significantly activated networks related to pro-inflammatory splenic Ly6C^{Hi} monocytes from SOD1 mice are shown: SP-1, NF-κB and CREB1. **(B)** Legend of network objects. For biological interpretation of the differentially expressed genes, software tool MetaCore™ (GeneGo) was used.

Supplemental Figure 4. Microglial loss occurs during disease progression in the spinal cord of SOD1 mice

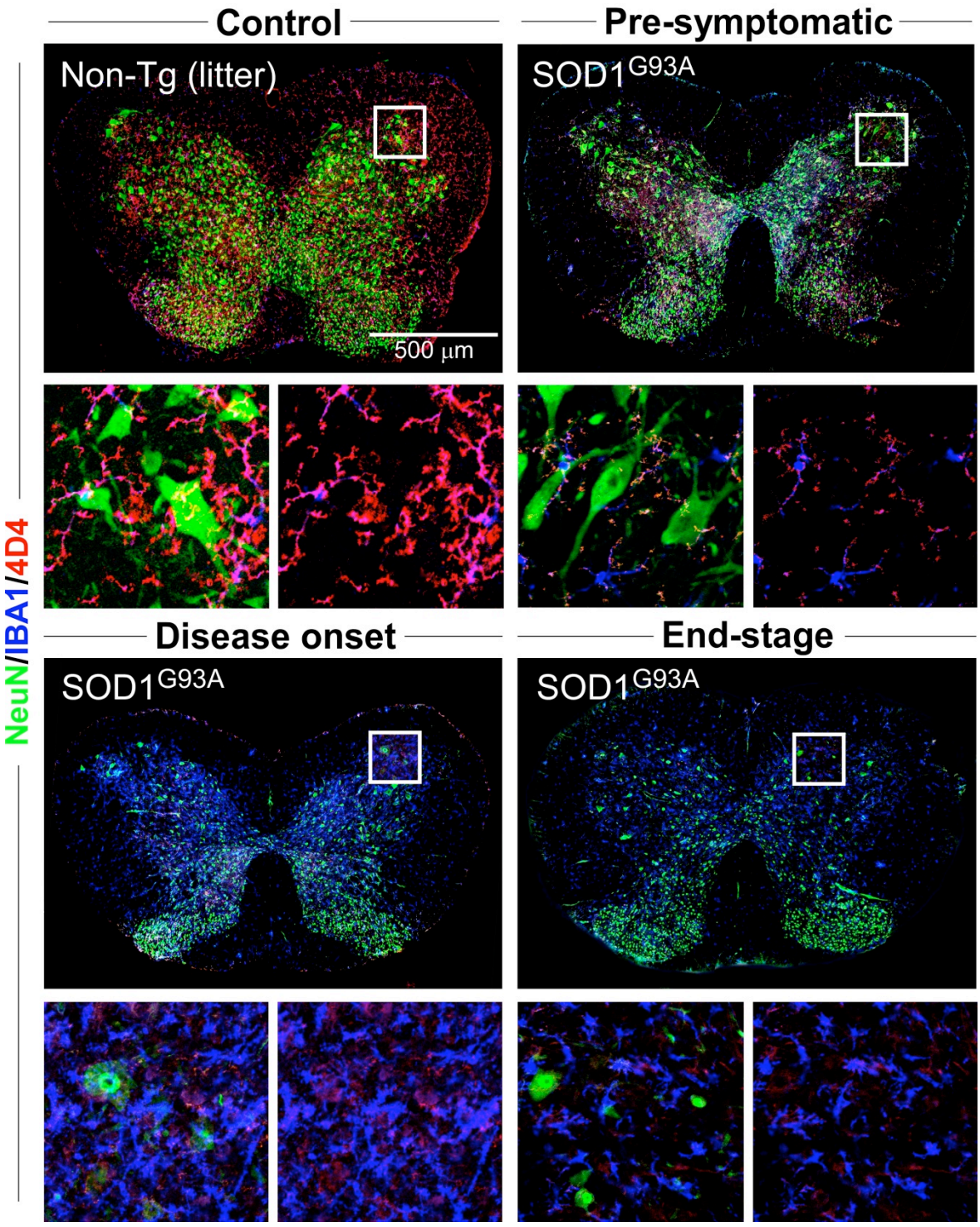

Supplemental Figure 4. Microglial loss occurs during disease progression in the spinal cord of SOD1 mice. Representative confocal images of whole mount axial sections of spinal cord from Non-Tg (litter) and SOD1^{G93A} transgenic B6/SJL mice at presymptomatic, disease onset and end-stage, as indicated. Immunohistochemistry of triple staining for 4D4 (a mAb with the identical specificity as CD39 to distinguish resident microglia from recruited peripheral macrophages/monocytes), NeuN (neurons) and IBA1 (stains both microglia and peripheral monocytes). Boxed areas represent inserts at high magnification in separate confocal channels.

Supplemental Figure 5. Ly6C and CD169 expression defines distinct monocyte infiltrate from indigenous CD39+ microglia in SOD1 mice

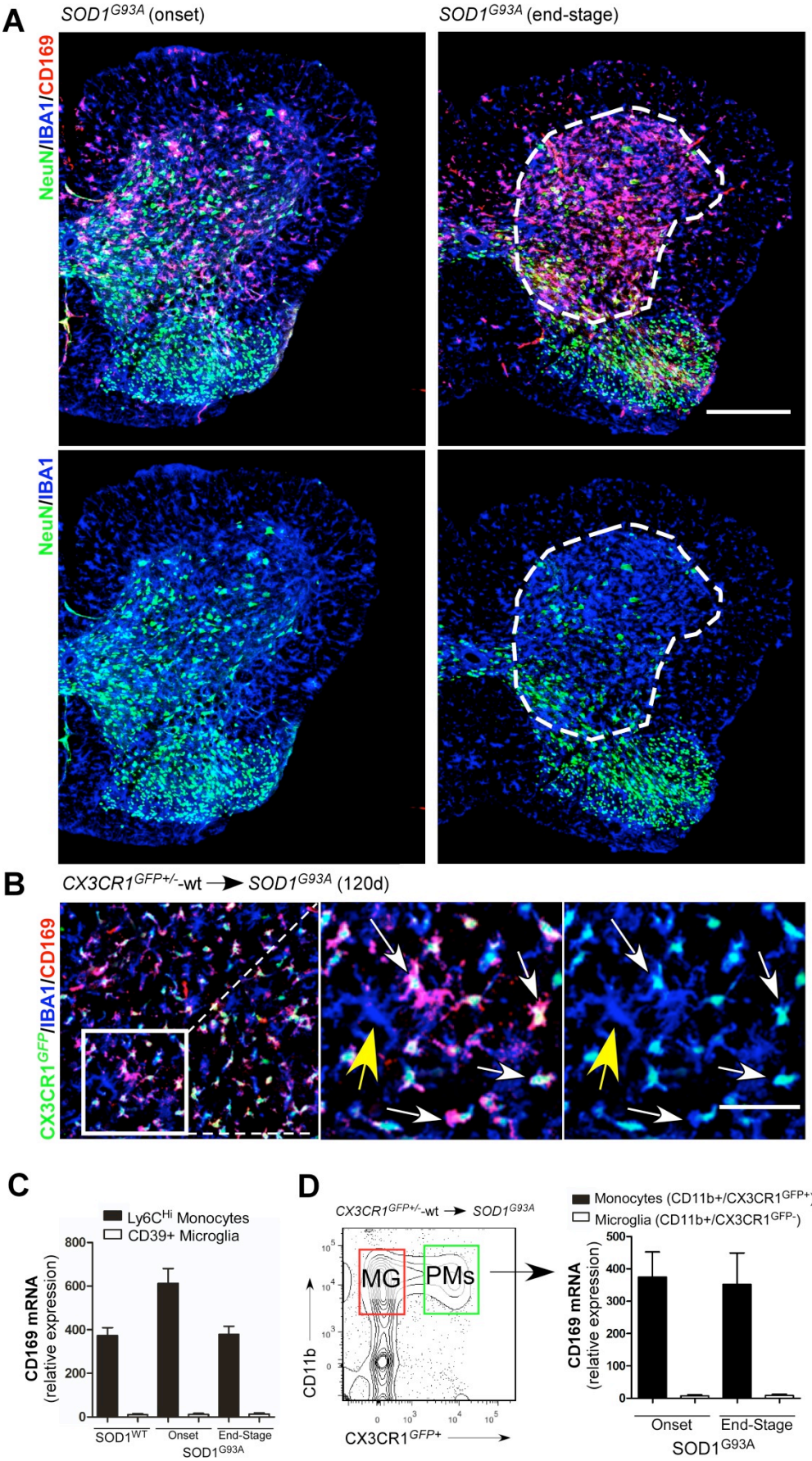

Supplemental Figure 5. Ly6C and CD169 expression distinguishes monocyte infiltrates from resident CD39^{+} microglia in SOD1 mice. (A) Fluorescence immunohistochemistry and confocal scanning laser microscopy of spinal cord axial sections from SOD1 at onset (defined by body-weight loss) and end-stage for NeuN (neuronal marker), IBA1 (myeloid marker) and CD169 (marker of inflammatory monocytes and differentiated dendritic cells ((7))) expression. Note, dashed line delineates area of CD169+ monocyte infiltrates and same area shown below of neuronal loss in the ventral horn at end-stage. Scale bar: 500 μm. **(B)** Spinal cords of SOD1-CX_3CR1-GFP$^{+/-}$ chimeric mice described in Figure 10 were analyzed for CD169 expression. Fluorescence immunohistochemistry and confocal scanning laser microscopy of spinal cord section of ventral horn from SOD1 chimeric CX3CR1$^{GFP/+}$ mouse at 120d stained for IBA (blue) and CD169 (red). Magnified boxed areas on the middle and right panels in separate laser channels show that all recruited monocytes (IBA1^{+}/GFP^{+}; white arrows) are positive for CD169 and that resident microglia (IBA1^{+}/GFP^{-}; yellow arrows) do not express CD169. Representative confocal images of 5 mice. Scale bar: 50 μm. **(C)** qRT-PCR analysis of *Siglec1* (CD169) mRNA expression in spinal cord-derived CD39^{+} microglia and spleen-derived Ly6C^{Hi} sorted by flow cytometry from wild type and SOD1^{G93A} mice at disease onset and end-stage. Total RNA was isolated and pooled from five mice. Expression levels were normalized to GAPDH. Note, CD169 expression was not detected in CD39^{+} microglia. Data represent mean ± SEM. **(D)** qRT-PCR analysis of *Siglec1* mRNA expression in spinal cord-derived microglia (MG; CD11b^{+}/GFP^{-}) and recruited peripheral BM-derived monocytes (PMs; CD11b^{+}/GFP^{+}) sorted by flow cytometry from SOD1 chimeric mice at onset and end-stage. Total RNA was isolated and pooled from three mice. Expression levels were normalized to GAPDH. Data represent mean ± SEM.

Supplemental Figure 6. Systemic treatment with anti-Ly6C mAb antibody reverses spleen atrophy in SOD1 mice

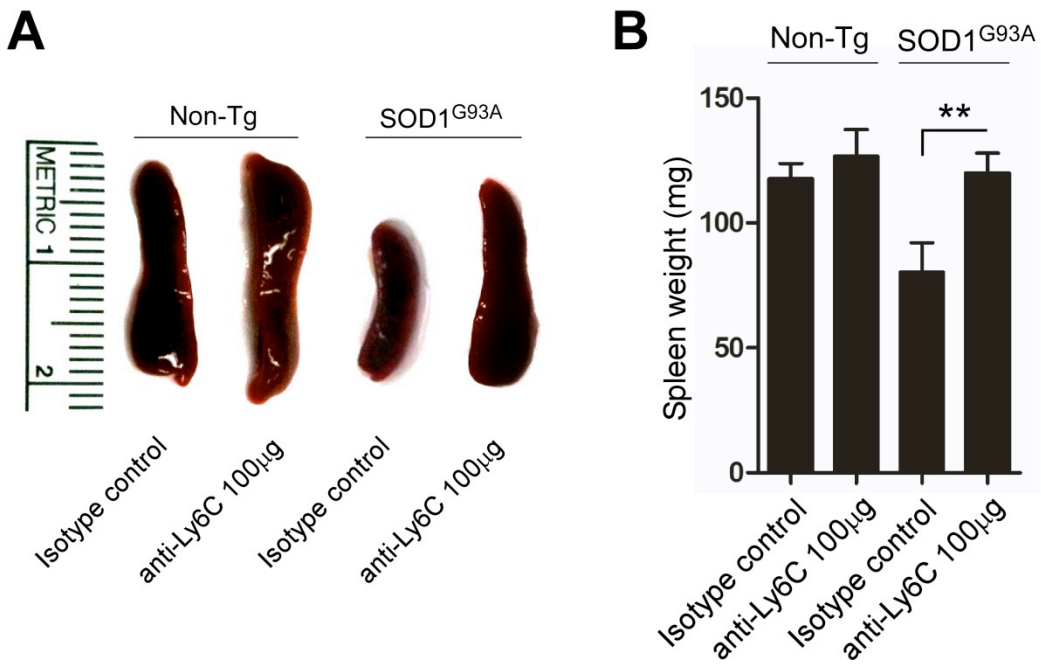

Supplemental Figure 6. Systemic treatment with anti-Ly6C mAb antibody reverses spleen atrophy in SOD1 mice. B6/SJL-SOD1^{G93A} and B6/SJL-Non-tg mice were treated as described in Figure 12. **(A)** Representative images of morphology and size of spleens from α-Ly6C-teated B6/SJL-SOD1^{G93A} and B6/SJL-Non-Tg compared to IC groups 30 days post-treatment (120d old). **(B)** Mean spleen weights were compared between B6/SJL-WT littermates and B6/SJL-SOD1 mice. Data represent mean ± SEM for 5-6 mice per group. $P < 0.01$ compared to IC control group by ANOVA with Bonferroni's post-hoc test.

Supplemental Fig. 7. Effect of splenectomy on survival and clinical scores in SOD1 mice

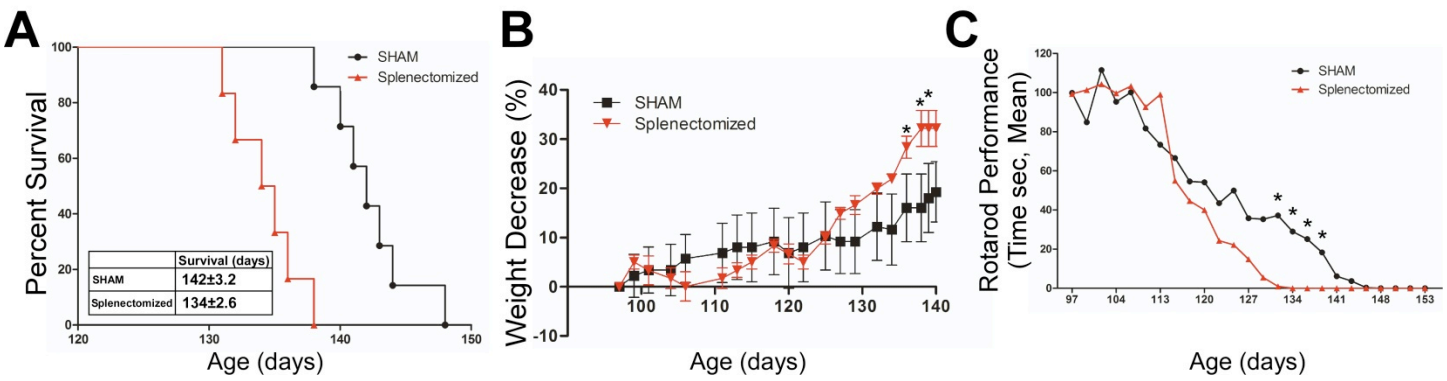

Supplemental Figure 7. **Effect of splenectomy on survival and clinical scores in SOD1 mice.** SOD1 mice were splenectomized at pre-symptomatic phase (60d old) (*n*=6). SHAM-operated SOD1 littermates (maintained and surgically operated under identical conditions as splenectomized mice, but without splenectomy) served as the control group (*n*=7). **(A)** Kaplan-Meir analysis of the probability of surviving of sham-operated and SOD1 splenectomized mice as a function of age. Log-rank (Mantel-Cox) test comparison showed significant differences (*P*=0.005). **(B)** Weight loss plotted for SHAM and splenectomized groups. Data represent mean ± SD. Statistical analysis between splenectomized and SHAM mice is by Student's *t* test (2-tailed). *P < 0.05. **(C)** Decline in rotarod performance of sham-operated and splenectomized mice as a function of age.

Supplemental Figure 8. CD14+/CD16- peripheral blood monocyte in ALS subjects

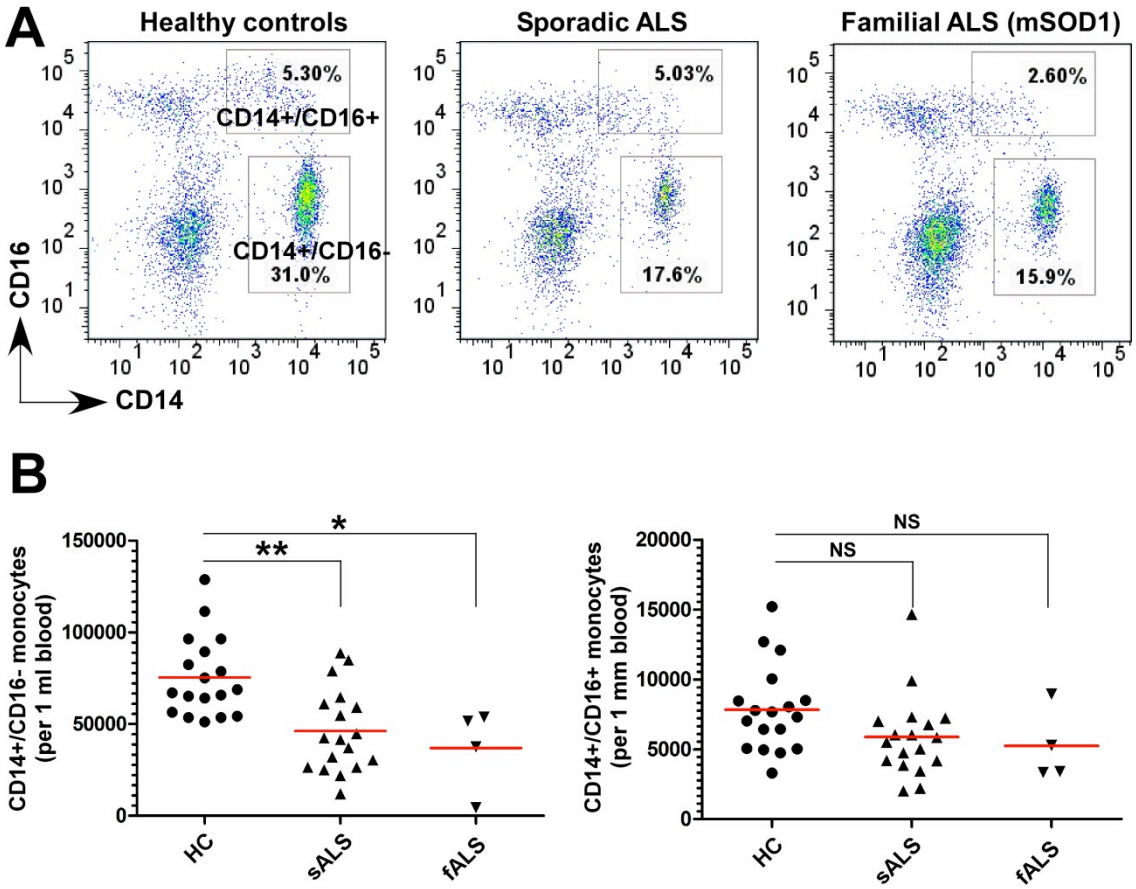

Supplemental Figure 8. CD14+/CD16- peripheral blood monocytes in ALS subjects. (A) Representative FACS histograms of CD14+/CD16- and CD14+/CD16+ monocyte subsets from peripheral blood of healthy controls, sporadic and familial ALS subjects. **(B)** Statistical analysis of absolute numbers of blood monocyte subsets in 1 ml of peripheral blood from healthy controls (*n*=18), sALS (*n*=18) and fALS (*n*=4) subjects which were used for miRNA and gene profiles shows a decrease in CD14+/CD16- monocytes. No statistically significant changes were observed for CD14+/CD16+ monocytes. Each data point indicates an individual subject. Horizontal bars denote mean of cell numbers in each group. Statistical analysis by one-way ANOVA followed by Dunnett's multiple-comparison post hoc test. *P < 0.05; **P < 0.01.

Supplemental Table 3. Similarly affected miRNAs and mRNAs in peripheral monocytes from SOD1 mice and sporadic and familial ALS subjects

Similar miRNAs	SOD1 mouse (Spleen-Ly6CHi)		sALS (Blood-CD14+/CD16-)		fALS (Blood-CD14+/CD16-)	
	Fold change	p-Value	Fold change	p-Value	Fold change	p-Value
let-7a	7.5	2.2E-02	2.8	3.3E-05	NT	NT
let-7b	2.8	4.6E-02	2.0	5.2E-05	NT	NT
let-7f	6.6	1.6E-02	2.1	5.2E-05	NT	NT
miR-103	1.8	5.0E-02	3.3	7.7E-06	NT	NT
miR-142-5p	1.5	3.5E-02	2.1	2.8E-07	7.5	1.8E-03
miR-146a	1.8	2.6E-02	4.2	9.8E-05	NT	NT
miR-15b	1.4	4.6E-02	2.1	2.8E-05	NT	NT
miR-155	3.1	6.8E-04	3.0	1.8E-04	7.0	4.6E-02
miR-16	1.9	1.9E-06	3.9	4.1E-08	NT	NT
miR-193	-3.4	9.0E-05	-2.1	6.2E-04	NT	NT
miR-19b	2.1	3.5E-03	3.1	7.6E-08	NT	NT
miR-223	2.0	9.4E-05	1.7	1.1E-02	6.4	5.0E-02
miR-26a	2.2	1.3E-03	4.4	8.7E-07	NT	NT
miR-26b	1.8	2.9E-02	2.4	6.1E-06	NT	NT
miR-27a	2.2	1.2E-02	4.2	1.2E-04	47.8	1.0E-03
miR-29a	2.0	2.7E-03	1.7	1.2E-03	NT	NT
miR-532-3p	1.8	2.7E-02	2.8	1.3E-06	4.9	1.0E-02
miR-574-3p	1.7	1.8E-06	2.1	1.5E-04	NT	NT
miR-93	1.4	1.4E-02	2.6	4.8E-05	NT	NT

Similar mRNAs	SOD1 mouse (Spleen-Ly6CHi)		sALS (Blood-CD14+/CD16-)		fALS (Blood-CD14+/CD16-)	
	Fold change	p-Value	Fold change	p-Value	Fold change	p-Value
AHR	5.2	8.9E-04	1.9	3.8E-04	2.0	6.0E-02
Mef2d	-3.2	2.1E-04	-1.5	1.5E-04	-1.5	4.4E-05
MHC-II	4.6	4.9E-05	1.3	4.4E-03	1.5	5.9E-03
Myc	3.9	7.2E-03	2.4	2.1E-02	2.2	1.6E-02
Nfkb1	2.8	1.6E-05	-1.2	3.8E-01	1.7	2.5E-06
Rac1	4.3	4.8E-07	1.3	2.2E-02	1.7	3.0E-02
Shc1	3.4	7.9E-05	1.4	1.6E-06	1.0	3.5E-01
SOCS1	-1.6	4.7E-02	-2.9	1.4E-07	-2.5	2.6E-03
Tgfb1	-4.0	5.7E-06	-1.6	7.8E-04	-1.4	6.7E-03
Tlr2	2.9	1.3E-04	1.3	2.7E-03	1.7	3.1E-02

Supplemental Table 3. Similarly affected miRNAs and inflammation-related genes in peripheral monocytes in SOD1 mice and sporadic and familial ALS subjects. Note, miRNA and gene expression in splenic Ly6C^{Hi} monocytes from SOD1 mice at disease onset. *Ahr* and *Socs1* genes were analyzed by qRT-PCR from WT (*n*=6) and SOD1^{G93A} (*n*=6) mice at disease onset. NT-not tested.

Supplementary Table 4. Significantly affected miRNAs in blood-derived CD14+/CD16- monocytes in MS and sALS subjects

Affected miRNAs	Fold change vs. HC		P value vs. HC	
Upregulated miRNAs	**MS**	**sALS**	**MS**	**sALS**
hsa-miR-26a	2.6	4.4	4.2E-05	2.4E-07
hsa-miR-146a	2.9	4.2	1.2E-03	3.6E-05
hsa-miR-27a	1.8	4.2	1.9E-02	1.4E-04
hsa-miR-16	2.4	3.9	1.0E-04	2.8E-08
hsa-miR-106b	1.6	3.8	5.4E-04	7.8E-10
hsa-miR-30b	1.9	3.6	1.8E-04	2.8E-08
hsa-miR-103	2.6	3.3	1.8E-05	2.9E-06
hsa-miR-374a	1.1	3.2	3.7E-01	5.7E-07
hsa-miR-19b	1.4	3.1	1.1E-03	1.6E-08
hsa-miR-24	2.2	3.0	4.5E-04	1.5E-06
hsa-miR-155	1.9	3.0	2.3E-03	8.1E-05
hsa-miR-532-3p	2.3	2.8	2.8E-04	3.2E-07
hsa-let-7a	2.5	2.8	1.8E-04	1.0E-05
hsa-miR-374b	1.5	2.7	9.7E-03	5.0E-07
hsa-miR-93	2.3	2.6	1.9E-06	2.6E-05
hsa-miR-21	-1.1	2.5	5.3E-01	2.0E-06
hsa-miR-1260	3.0	2.5	7.2E-05	7.2E-04
hsa-miR-361-5p	2.4	2.5	1.6E-04	3.8E-07
hsa-miR-27b	3.7	2.4	3.3E-05	1.1E-03
hsa-miR-26b	1.5	2.4	4.4E-03	6.1E-06
hsa-miR-101	-1.1	2.3	2.6E-01	1.2E-06
hsa-miR-20a	2.0	2.3	5.0E-05	7.1E-06
hsa-miR-720	2.7	2.3	4.3E-04	2.2E-02
hsa-miR-340	-1.4	2.2	8.4E-02	2.7E-05
hsa-let-7f	1.5	2.1	3.8E-03	1.7E-05
hsa-miR-574-3p	1.2	2.1	1.8E-01	6.6E-05
hsa-miR-423-3p	2.2	2.1	4.8E-05	1.3E-04
hsa-miR-15b	1.5	2.1	3.1E-02	1.0E-05
hsa-miR-142-5p	-1.1	2.1	2.7E-01	5.3E-07
hsa-miR-221	1.7	2.0	2.7E-04	1.4E-06
hsa-miR-320c	3.4	2.0	1.5E-04	1.0E-02
hsa-miR-30c	1.8	2.0	1.2E-03	9.9E-04
hsa-let-7b	2.2	2.0	1.5E-04	1.7E-05
hsa-miR-19a	1.0	2.0	9.7E-01	1.4E-04
hsa-miR-664	2.6	1.9	4.3E-05	1.7E-03
hsa-miR-29c	-1.3	1.8	1.8E-01	1.2E-03
hsa-miR-29a	-1.1	1.7	4.5E-01	5.3E-04
hsa-miR-223	1.0	1.7	8.7E-01	5.6E-03
hsa-miR-423-5p	2.3	1.6	1.3E-05	1.8E-03
hsa-miR-197	2.2	1.3	9.2E-04	1.1E-01
Downregulated miRNAs	**MS**	**sALS**	**MS**	**sALS**
hsa-miR-660	-2.2	-1.7	3.9E-03	2.7E-02
hsa-miR-453	-1.2	-1.9	9.0E-02	1.6E-05
hsa-miR-526a	-1.3	-1.9	5.2E-02	2.1E-04
hsa-miR-598	-1.9	-2.0	2.3E-04	1.4E-04
hsa-miR-603	-1.3	-2.0	4.1E-02	1.8E-04
hsa-miR-651	-1.4	-2.0	6.8E-03	5.1E-05
hsa-miR-193a-3p	-1.6	-2.1	3.9E-03	2.4E-04
hsa-miR-548g	-1.5	-2.1	3.0E-03	3.4E-05
hsa-miR-379	-1.5	-2.1	4.3E-03	3.2E-05
hsa-miR-137	-1.5	-2.1	9.9E-03	1.4E-04
hsa-miR-383	-2.0	-2.1	6.3E-04	9.6E-04
hsa-miR-649	-2.1	-2.2	2.7E-03	2.5E-03
hsa-miR-1297	-1.3	-2.2	5.7E-02	1.8E-05
hsa-miR-1206	-1.6	-2.2	1.8E-03	8.7E-05
hsa-miR-302c	-1.9	-2.3	8.3E-03	2.5E-03
hsa-miR-513a-5p	-1.9	-2.5	1.9E-03	1.7E-04

Supplemental Table 4. **Significantly affected miRNAs in blood-derived CD14+/CD16- monocytes in MS and sALS subjects.** Note, values represent fold change of significantly up or downregulated miRNAs in MS (*n*=8) and sALS (*n*=8) subjects from HC subjects (*n*=8). Total RNA was isolated from sorted blood-derived CD14+/CD16- monocytes (Supplemental Figure 8). *P* values represent statistical differences between 2 groups by Student's t test (2-tailed).

Supplemental Figure 9. Expression of miRNAs in CD14+/CD16+ blood monocytes in ALS and MS subjects

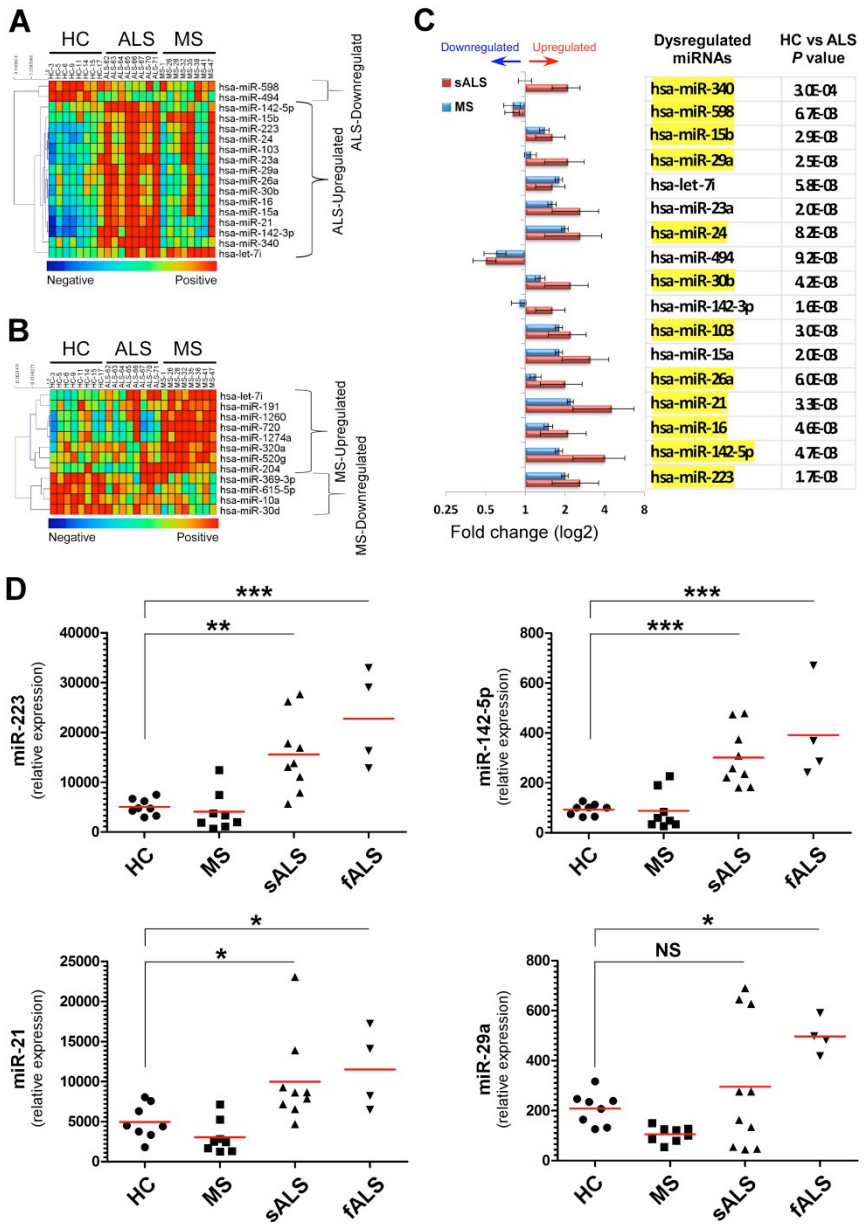

Supplemental Figure 9. Expression of miRNAs in CD14$^+$/CD16$^+$ blood monocytes in ALS and MS subjects. Quantitative nCounter expression profiling of blood-derived CD14$^+$/CD16$^+$ monocytes for 664 miRNAs in sporadic ALS (*n*=8) and relapsing-remitting MS (*n*=8) compared to healthy controls (*n*=8) from the same subjects shown in Figure 15. Heatmap hierarchical clustering (Pearson correlation) shows significantly affected miRNAs in **(A)** ALS and **(B)** MS subjects with at least 2-fold altered transcription levels (Nonparametric Kruskal-Wallis test, significance based on FDR Benjamini-Hochberg; selected FDR limit: 0.05; P<0.01). Uncentered Pearson correlation was used as the distance metric with average linkage for the unsupervised hierarchical clustering. **(C)** Summary of significantly affected miRNAs in ALS subjects. Note, bars show fold differences of significantly affected miRNAs in ALS subjects from healthy controls. miRNA expression level has been normalized against the geometric mean of five house-keeping genes (*ACTB, B2M, GAPDH, RPL19, RPLP0*). Note, 70% of the identified affected miRNAs in CD14$^+$/CD16$^+$ blood monocytes in ALS (12 miRNAs highlighted in yellow) were identical to miRNAs affected in CD14$^+$/CD16$^-$ blood monocytes from the same ALS subjects (see Figure 15). **(D)** qRT-PCR validation of 4 selected miRNAs in an independent HC (*n*=8) and sALS (*n*=9-10) cohort. Relative expression in HC, MS, sALS and fALS were calculated using the comparative Ct (2−ΔΔCt) method. miRNA expression level was normalized against U6 miRNA. PCRs were run in duplicates per subject. The graphs represent one-way ANOVA and the Dunnett's multiple comparison tests of significantly upregulated miRNAs in ALS subjects. Each data point indicates an individual subject. Horizontal bars denote mean of miRNA expression in each group. *P < 0.05; **P < 0.01; ***P < 0.001.

Supplemental Figure 10. Expression of miRNAs in CSF of ALS subjects

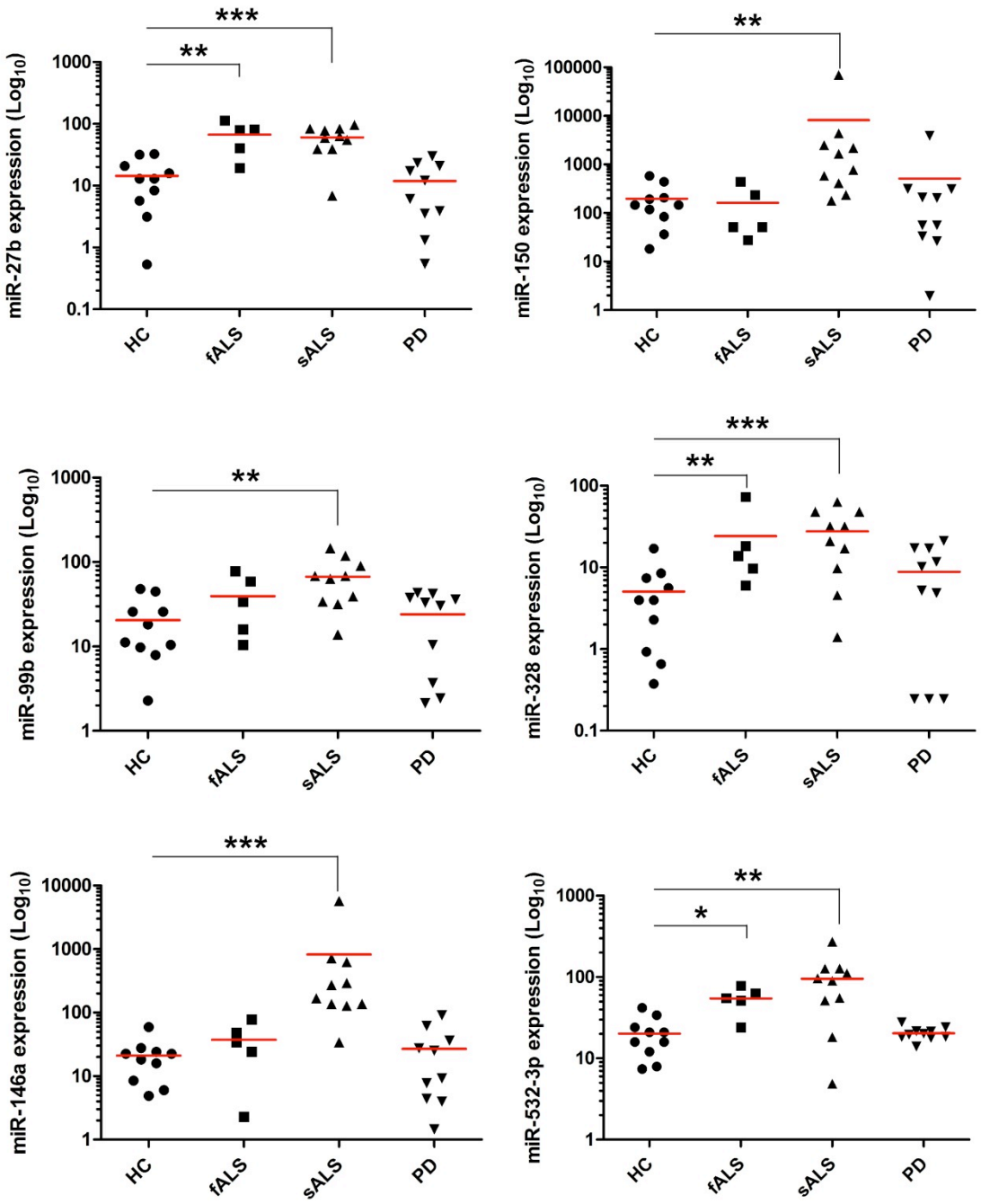

Supplemental Figure 10. **Expression of miRNAs in CSF of ALS subjects.** Cerebrospinal fluid (CSF) from healthy controls (HC; *n*=10), sporadic ALS (sALS; *n*=10), familial ALS (fALS; *n*=5) and Parkinson disease (PD; *n*=10) subjects was examined for 43 selected microRNAs which we found upregulated in splenic Ly6C^{Hi} monocytes (see Figure 4A) and SOD1 spinal cord CD39^{+} microglia (see Figure 6A). 6 miRNAs (miR-27b, miR-150, miR-99b, miR-328, miR-146a and miR-532-3p) were significantly upregulated in sALS or fALS subjects. Note, no differential expression of these miRNA was detected in PD subjects. Relative expression in HC, fALS, sALS and PD were calculated using the comparative Ct ($2^{-\Delta\Delta Ct}$) method. miRNA expression level was normalized against miR-125b miRNA (see *Methods*). PCRs were run in duplicates per subject. The graphs represent one-way ANOVA and the Dunnett's multiple comparison tests of significantly upregulated miRNAs in ALS subjects. Each data point indicates an individual subject. Horizontal bars denote mean of miRNA expression in each group. *P < 0.05; **P < 0.01; ***P < 0.001.

Supplemental Figure 11. Inflammation-related gene profiling in CD14+/CD16- blood monocytes in ALS and MS subjects

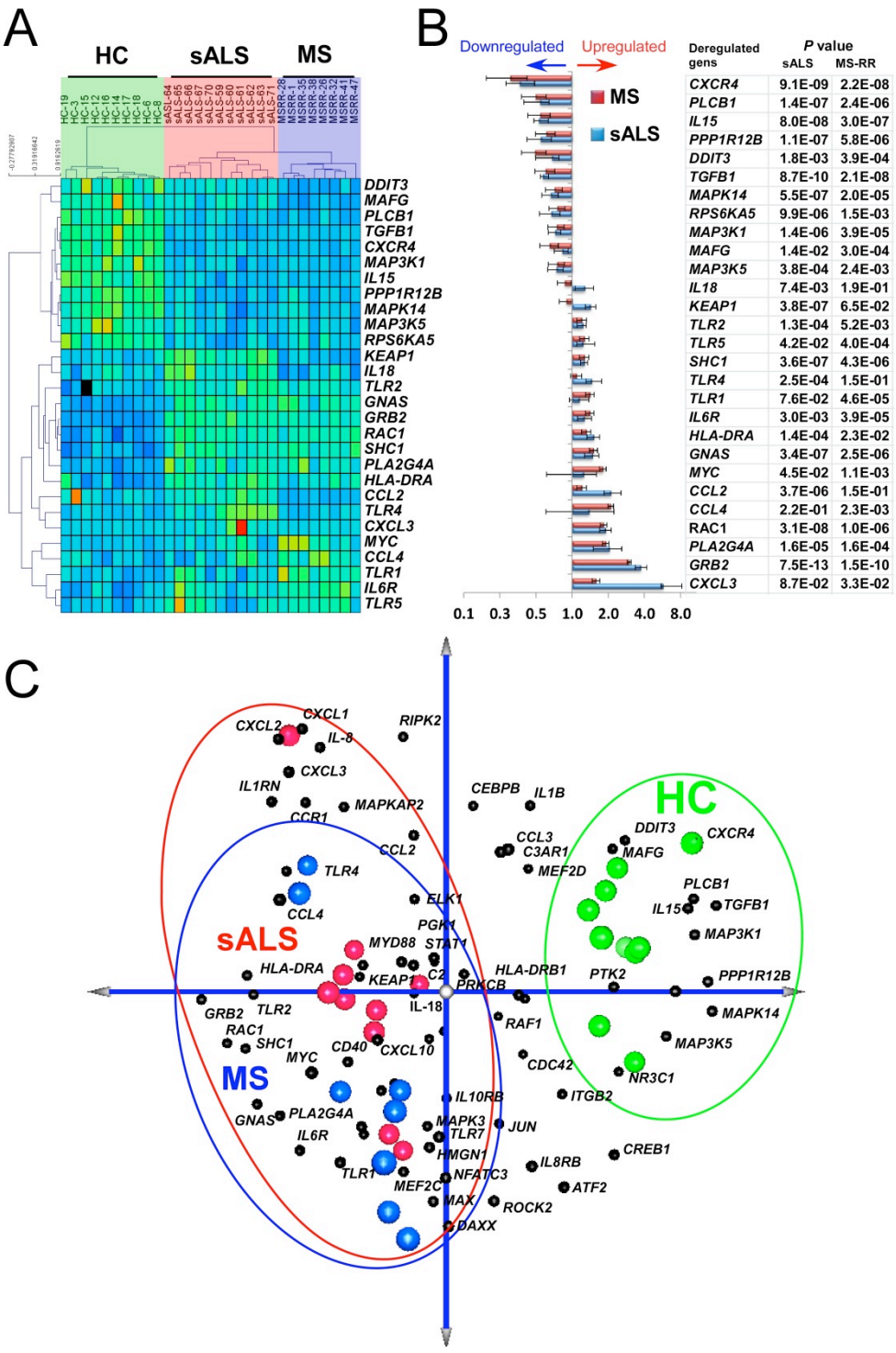

Deregulated gens	*P* value sALS	MS-RR
CXCR4	9.1E-09	2.2E-08
PLCB1	1.4E-07	2.4E-06
IL15	8.0E-08	3.0E-07
PPP1R12B	1.1E-07	5.8E-06
DDIT3	1.8E-03	3.9E-04
TGFB1	8.7E-10	2.1E-08
MAPK14	5.5E-07	2.0E-05
RPS6KA5	9.9E-06	1.5E-03
MAP3K1	1.4E-06	3.9E-05
MAFG	1.4E-02	3.0E-04
MAP3K5	3.8E-04	2.4E-03
IL18	7.4E-03	1.9E-01
KEAP1	3.8E-07	6.5E-02
TLR2	1.3E-04	5.2E-03
TLR5	4.2E-02	4.0E-04
SHC1	3.6E-07	4.3E-06
TLR4	2.5E-04	1.5E-01
TLR1	7.6E-02	4.6E-05
IL6R	3.0E-03	3.9E-05
HLA-DRA	1.4E-04	2.3E-02
GNAS	3.4E-07	2.5E-06
MYC	4.5E-02	1.1E-03
CCL2	3.7E-06	1.5E-01
CCL4	2.2E-01	2.3E-03
RAC1	3.1E-08	1.0E-06
PLA2G4A	1.6E-05	1.6E-04
GRB2	7.5E-13	1.5E-10
CXCL3	8.7E-02	3.3E-02

Supplemental Figure 11. Inflammation-related gene profiling in CD14^{+}/CD16^{-} blood monocytes in ALS and MS subjects. (A) nCounter expression profiles of 184 inflammation-related genes in CD14^{+}/CD16^{-} blood monocytes from ALS (*n*=8) and MS (*n*=11) subjects compared to healthy controls (*n*=10). **(B)** Bars show fold differences of significantly affected genes in sALS and MS subjects from healthy controls. Data represent mean ± SD. Gene expression level has been normalized against geometric mean of 6 internal reference house-keeping genes (*CLTC, GAPDH, GUSB, HPRT1, PGK1, TUBB5*). **(C)** PCA analysis of the identified affected genes between sALS and MS subjects with spatial gene distribution.

Supplementary Table 5. Significantly affected immune-related genes in blood-derived CD14+/CD16- monocytes in sALS and fALS subjects

Affected genes	Fold change vs. HC		P value vs. HC	
Upregulated genes	sALS	fALS	sALS	fALS
CCL2	9.2	18.4	1.7E-02	2.5E-03
FCER1A	0.8	7.3	5.2E-01	2.1E-04
CSF1	4.7	7.2	3.1E-02	3.4E-02
CXCL3	4.1	5.4	6.5E-04	8.2E-02
CCL4	2.3	3.9	4.2E-02	8.7E-02
CCR1	1.8	3.0	3.9E-02	9.4E-06
IL7R	-1.2	2.3	1.2E-01	2.3E-01
MYC	2.4	2.2	2.1E-02	1.6E-02
PTAFR	1.9	2.1	3.2E-05	3.4E-02
IL1RN	1.9	2.1	5.8E-02	4.9E-03
TNFSF14	2.2	2.1	7.0E-02	1.3E-01
AHR	1.9	2.0	3.8E-04	6.0E-02
LILRB4	-1.4	1.8	1.3E-01	1.3E-03
TLR2	1.3	1.7	2.7E-03	3.1E-02
RAC1	1.3	1.7	2.2E-02	3.0E-02
JAK3	1.7	1.7	6.6E-03	4.6E-02
KLRB1	-1.3	1.7	3.6E-02	2.7E-01
SELL	-1.3	1.5	7.6E-02	3.3E-02
HLA-DRA	1.3	1.5	4.4E-03	5.9E-03
ITGAM	1.4	1.5	1.7E-08	5.0E-02
TNFSF8	1.8	1.5	3.4E-02	3.6E-01
CD82	1.7	1.4	7.3E-03	1.9E-01
CD81	-2.0	1.4	2.5E-03	1.9E-02
NFKB1	-1.2	1.4	3.8E-01	7.7E-03
RUNX1	1.5	1.3	1.9E-02	2.6E-01
IL6R	1.3	1.3	1.8E-02	7.2E-02
IL4R	1.4	1.3	8.0E-04	3.7E-02
CD44	1.6	1.2	9.3E-03	3.4E-01
TLR4	1.3	1.2	7.3E-04	1.5E-02
FCER1G	-1.2	1.1	3.7E-02	1.2E-01
TRAF3	1.7	1.1	4.5E-03	5.5E-01
BCL3	1.8	1.1	5.1E-03	7.4E-01
LIMK1	1.6	1.1	1.8E-02	4.7E-01
SHC1	1.4	1.0	1.6E-06	3.5E-01
KEAP1	1.5	-1.2	9.0E-03	1.5E-01
IL18	1.3	-1.3	2.2E-02	1.9E-03
TGFB1	-1.6	-1.4	7.8E-04	6.7E-03
CASP10	-1.5	-1.4	3.0E-04	2.0E-01
RIPK2	-2.1	-1.5	7.3E-06	6.5E-04
MEF2D	-1.5	-1.5	1.5E-04	4.4E-05
LTB4R	1.1	-1.6	3.3E-01	1.9E-04
CDKN1A	-1.4	-1.6	1.3E-03	1.0E-01
PLAUR	-2.5	-1.6	2.9E-05	2.2E-01
CD83	-1.4	-1.6	2.2E-02	1.5E-01
LITAF	-1.6	-1.6	2.2E-03	1.2E-01
TNFRSF8	-1.5	-1.6	9.7E-03	2.8E-03
LCP2	-1.7	-1.7	9.9E-06	9.0E-04
PTK2	-1.4	-1.9	2.9E-02	3.0E-04
NFKBIZ	-1.7	-1.9	3.6E-05	6.9E-03
NFE2L2	-2.0	-1.9	4.5E-09	9.3E-06
FOS	-1.8	-2.0	5.0E-04	4.0E-02
DDIT3	-1.3	-2.0	3.6E-02	3.0E-05
LILRA5	-1.5	-2.0	1.6E-02	4.0E-03
PTGS2	-2.5	-2.1	3.7E-05	1.0E-03
PRDM1	-2.3	-2.2	6.7E-04	3.7E-02
TAGAP	-2.2	-2.3	4.5E-07	7.1E-04
SOCS1	-2.9	-2.5	1.4E-07	2.6E-03
NCR1	-3.3	-3.4	1.9E-05	1.4E-04
CXCR4	-3.9	-4.2	5.7E-10	2.1E-09

Supplemental Table 5. **Significantly affected immune-related genes in blood-derived CD14+/CD16- monocytes in sALS and fALS subjects.** Note, values represent fold change of significantly up or downregulated miRNAs in sALS (*n*=10) and fALS (*n*=4) subjects from HC subjects (*n*=10). *P* values represent statistical differences between 2 groups by Student's t test (2-tailed).

Supplementary Table 6. MicroRNA target filter analysis identified 32 miRNAs targeting 27 mRNAs in ALS subjects

ID	Symbol	Fold Change	Symbol	Fold Change	Expression Pairing	Source	Confidence
hsa-miR-137	miR-137 (human, mouse, rat)	↓-2.100	AHR	↑2.000	↓↑	TargetScan Human	High (predicted)
hsa-miR-302c	miR-302a/miR-302b/miR-291a-3p (includes others	↓-2.300	AHR	↑2.000	↓↑	TargetScan Human	High (predicted)
hsa-miR-453	miR-410*/miR-494*/miR-496* (includes others	↓-1.900	AHR	↑2.000	↓↑	TargetScan Human	Moderate (predicted)
hsa-miR-19b	miR-19b/miR-19a	↑3.100	CASP10	↓-1.500	↑↓	TargetScan Human	Moderate (predicted)
hsa-miR-24	miR-24	↑3.000	CASP10	↓-1.500	↑↓	TargetScan Human	Moderate (predicted)
hsa-miR-361-5p	miR-361/miR-361-5p	↑2.500	CASP10	↓-1.500	↑↓	TargetScan Human	Moderate (predicted)
hsa-miR-302c	miR-302a/miR-302b/miR-291a-3p (includes others	↓-2.300	CD44	↑1.600	↓↑	TargetScan Human, miRecords	Experimentally Observed,High (predicted)
hsa-miR-513a-5p	miR-513a-5p	↓-2.500	CD44	↑1.600	↓↑	TargetScan Human	Moderate (predicted)
hsa-miR-526a	miR-526a/miR-522*/miR-520c-5p (includes others	↓-1.900	CD44	↑1.600	↓↑	TargetScan Human	Moderate (predicted)
hsa-let-7a	let-7a/let-7f/let-7c (includes others)	↑2.800	CDKN1A	↓-1.400	↑↓	TargetScan Human	High (predicted)
hsa-miR-106b	miR-20a/miR-106b/miR-17-5p (includes others	↑3.800	CDKN1A	↓-1.400	↑↓	Ingenuity Expert Findings, TarBase, TargetScan Human, miRecords	Experimentally Observed,High (predicted)
hsa-miR-21	miR-21/miR-590-5p	↑2.500	CDKN1A	↓-1.400	↑↓	miRecords	Experimentally Observec
hsa-miR-423-5p	miR-423-5p/miR-423*/miR-3573-5p (includes others	↑1.600	CDKN1A	↓-1.400	↑↓	TargetScan Human	Moderate (predicted)
hsa-miR-603	miR-603/miR-3571	↓-2.000	CXCL3	↑5.400	↓↑	TargetScan Human	Moderate (predicted)
hsa-miR-146a	miR-146a/miR-146b/miR-146b-5p	↑4.200	CXCR4	↓-4.200	↑↓	miRecords	Experimentally Observec
hsa-miR-101	miR-101/miR-101a/miR-101b	↑2.300	FOS	↓-2.000	↑↓	TargetScan Human	High (predicted)
hsa-miR-155	miR-155 (human, mouse)	↑3.000	FOS	↓-2.000	↑↓	TargetScan Human	High (predicted)
hsa-miR-221	miR-222/miR-221/miR-192b	↑2.000	FOS	↓-2.000	↑↓	TargetScan Human, miRecords	Experimentally Observed,High (predicted)
hsa-miR-29c	miR-29b/miR-29c/miR-29a	↑1.800	FOS	↓-2.000	↑↓	TargetScan Human	High (predicted)
hsa-miR-374a	miR-374/miR-374a/miR-374b	↑3.200	FOS	↓-2.000	↑↓	TargetScan Human	Moderate (predicted)
hsa-miR-513a-5p	miR-513a-5p	↓-2.500	IL1RN	↑2.100	↓↑	TargetScan Human	Moderate (predicted)
hsa-miR-603	miR-603/miR-3571	↓-2.000	ITGAM	↑1.500	↓↑	TargetScan Human	High (predicted)
hsa-miR-16	miR-16/miR-497/miR-195 (includes others)	↑3.900	LITAF	↓-1.600	↑↓	TargetScan Human	High (predicted)
hsa-miR-106b	miR-20a/miR-106b/miR-17-5p (includes others	↑3.800	LITAF	↓-1.600	↑↓	TargetScan Human	High (predicted)
hsa-miR-27a	miR-27b/miR-27a	↑4.200	LITAF	↓-1.600	↑↓	TargetScan Human	High (predicted)
hsa-miR-24	miR-24	↑3.000	LTB4R	↓-1.600	↑↓	TargetScan Human	Moderate (predicted)
hsa-miR-320c	miR-320d/miR-320b/miR-320c (includes others	↑2.000	LTB4R	↓-1.600	↑↓	TargetScan Human	Moderate (predicted)
hsa-let-7a	let-7a/let-7f/let-7c (includes others)	↑2.800	MEF2D	↓-1.500	↑↓	TargetScan Human	High (predicted)
hsa-miR-101	miR-101/miR-101a/miR-101b	↑2.300	MEF2D	↓-1.500	↑↓	TargetScan Human	High (predicted)
hsa-miR-19b	miR-19b/miR-19a	↑3.100	MEF2D	↓-1.500	↑↓	TargetScan Human	High (predicted)
hsa-miR-106b	miR-20a/miR-106b/miR-17-5p (includes others	↑3.800	MEF2D	↓-1.500	↑↓	miRecords	Experimentally Observec
hsa-miR-223	miR-223	↑1.700	MEF2D	↓-1.500	↑↓	TargetScan Human	High (predicted)
hsa-miR-30b	miR-30c/miR-30a/miR-30d (includes others)	↑3.600	MEF2D	↓-1.500	↑↓	TargetScan Human	High (predicted)
hsa-miR-374a	miR-374/miR-374a/miR-374b	↑3.200	MEF2D	↓-1.500	↑↓	TargetScan Human	High (predicted)
hsa-miR-423-5p	miR-423-5p/miR-423*/miR-3573-5p (includes others	↑1.600	MEF2D	↓-1.500	↑↓	TargetScan Human	Moderate (predicted)
hsa-miR-1260	miR-1260b/miR-126(	↑2.500	NCR1	↓-3.400	↑↓	TargetScan Human	Moderate (predicted)
hsa-miR-532-3p	miR-532-3p	↑2.800	NCR1	↓-3.400	↑↓	TargetScan Human	Moderate (predicted)
hsa-miR-101	miR-101/miR-101a/miR-101b	↑2.300	NFE2L2	↓-2.000	↑↓	TargetScan Human	Moderate (predicted)
hsa-miR-142-5p	miR-142-5p	↑2.100	NFE2L2	↓-2.000	↑↓	TargetScan Human	High (predicted)
hsa-miR-27a	miR-27b/miR-27a	↑4.200	NFE2L2	↓-2.000	↑↓	TargetScan Human	Moderate (predicted)
hsa-miR-340	miR-340-5p/miR-34(	↑2.200	NFE2L2	↓-2.000	↑↓	TargetScan Human	High (predicted)
hsa-miR-374a	miR-374/miR-374a/miR-374b	↑3.200	NFKBIZ	↓-1.900	↑↓	TargetScan Human	High (predicted)
hsa-miR-142-5p	miR-142-5p	↑2.100	PLAUR	↓-2.500	↑↓	TargetScan Human	High (predicted)
hsa-miR-340	miR-340-5p/miR-34(	↑2.200	PLAUR	↓-2.500	↑↓	TargetScan Human	High (predicted)
hsa-let-7a	let-7a/let-7f/let-7c (includes others)	↑2.800	PRDM1	↓-2.300	↑↓	Ingenuity Expert Findings, TargetScan Human, miRecords	Experimentally Observed,High (predicted)
hsa-miR-223	miR-223	↑1.700	PRDM1	↓-2.300	↑↓	TargetScan Human	High (predicted)
hsa-miR-30b	miR-30c/miR-30a/miR-30d (includes others)	↑3.600	PRDM1	↓-2.300	↑↓	TargetScan Human	High (predicted)
hsa-miR-320c	miR-320d/miR-320b/miR-320c (includes others	↑2.000	PRDM1	↓-2.300	↑↓	TargetScan Human	Moderate (predicted)
hsa-miR-340	miR-340-5p/miR-34(	↑2.200	PRDM1	↓-2.300	↑↓	TargetScan Human	High (predicted)
hsa-miR-374a	miR-374/miR-374a/miR-374b	↑3.200	PRDM1	↓-2.300	↑↓	TargetScan Human	High (predicted)
hsa-miR-1206	miR-120(	↓-2.200	PTAFR	↑2.100	↓↑	TargetScan Human	Moderate (predicted)
hsa-let-7a	let-7a/let-7f/let-7c (includes others)	↑2.800	PTGS2	↓-2.500	↑↓	TarBase	Experimentally Observec
hsa-miR-101	miR-101/miR-101a/miR-101b	↑2.300	PTGS2	↓-2.500	↑↓	TargetScan Human, miRecords	Experimentally Observed,High (predicted)
hsa-miR-146a	miR-146a/miR-146b/miR-146b-5p	↑4.200	PTGS2	↓-2.500	↑↓	TargetScan Human	Moderate (predicted)
hsa-miR-16	miR-16/miR-497/miR-195 (includes others)	↑3.900	PTGS2	↓-2.500	↑↓	TarBase	Experimentally Observec
hsa-miR-26a	miR-26a/miR-26b	↑4.400	PTGS2	↓-2.500	↑↓	TargetScan Human	High (predicted)
hsa-miR-340	miR-340-5p/miR-34(	↑2.200	PTGS2	↓-2.500	↑↓	TargetScan Human	Moderate (predicted)
hsa-miR-374a	miR-374/miR-374a/miR-374b	↑3.200	PTGS2	↓-2.500	↑↓	TargetScan Human	High (predicted)
hsa-miR-664	miR-664 (human, mouse, rat)	↑1.900	PTGS2	↓-2.500	↑↓	TargetScan Human	High (predicted)
hsa-miR-221	miR-222/miR-221/miR-192b	↑2.000	PTK2	↓-1.900	↑↓	TargetScan Human	Moderate (predicted)
hsa-miR-340	miR-340-5p/miR-34(	↑2.200	PTK2	↓-1.900	↑↓	TargetScan Human	High (predicted)
hsa-miR-137	miR-137 (human, mouse, rat)	↓-2.100	RAC1	↑1.700	↓↑	TargetScan Human	High (predicted)
hsa-miR-302c	miR-302a/miR-302b/miR-291a-3p (includes others	↓-2.300	RUNX1	↑1.500	↓↑	TargetScan Human	High (predicted)
hsa-miR-513a-5p	miR-513a-5p	↓-2.500	RUNX1	↑1.500	↓↑	TargetScan Human	Moderate (predicted)
hsa-miR-548g	miR-548g	↓-2.100	RUNX1	↑1.500	↓↑	TargetScan Human	High (predicted)
hsa-miR-603	miR-603/miR-3571	↓-2.000	SELL	↑1.500	↓↑	TargetScan Human	Moderate (predicted)
hsa-let-7a	let-7a/let-7f/let-7c (includes others)	↑2.800	SOCS1	↓-2.900	↑↓	TargetScan Human	Moderate (predicted)
hsa-miR-142-5p	miR-142-5p	↑2.100	SOCS1	↓-2.900	↑↓	TargetScan Human	Moderate (predicted)
hsa-miR-155	miR-155 (human, mouse)	↑3.000	SOCS1	↓-2.900	↑↓	Ingenuity Expert Findings, TargetScan Human, miRecords	Experimentally Observed,High (predicted)
hsa-miR-19b	miR-19b/miR-19a	↑3.100	SOCS1	↓-2.900	↑↓	TargetScan Human	High (predicted)
hsa-miR-221	miR-222/miR-221/miR-192b	↑2.000	SOCS1	↓-2.900	↑↓	TargetScan Human	High (predicted)
hsa-miR-30b	miR-30c/miR-30a/miR-30d (includes others)	↑3.600	SOCS1	↓-2.900	↑↓	TargetScan Human	High (predicted)
hsa-miR-106b	miR-20a/miR-106b/miR-17-5p (includes others	↑3.800	TAGAP	↓-2.300	↑↓	TargetScan Human	High (predicted)
hsa-miR-21	miR-21/miR-590-5p	↑2.500	TAGAP	↓-2.300	↑↓	TargetScan Human	High (predicted)
hsa-miR-374a	miR-374/miR-374a/miR-374b	↑3.200	TAGAP	↓-2.300	↑↓	TargetScan Human	Moderate (predicted)
hsa-miR-526a	miR-526a/miR-522*/miR-520c-5p (includes others	↓-1.900	TLR2	↑1.700	↓↑	TargetScan Human	Moderate (predicted)
hsa-miR-603	miR-603/miR-3571	↓-2.000	TLR4	↑1.600	↓↑	TargetScan Human	High (predicted)

Supplemental Table 6. microRNA-mRNA target filter analysis (IPA; Ingenuity) identified 32 miRNAs targeting 27 mRNAs in ALS subjects.

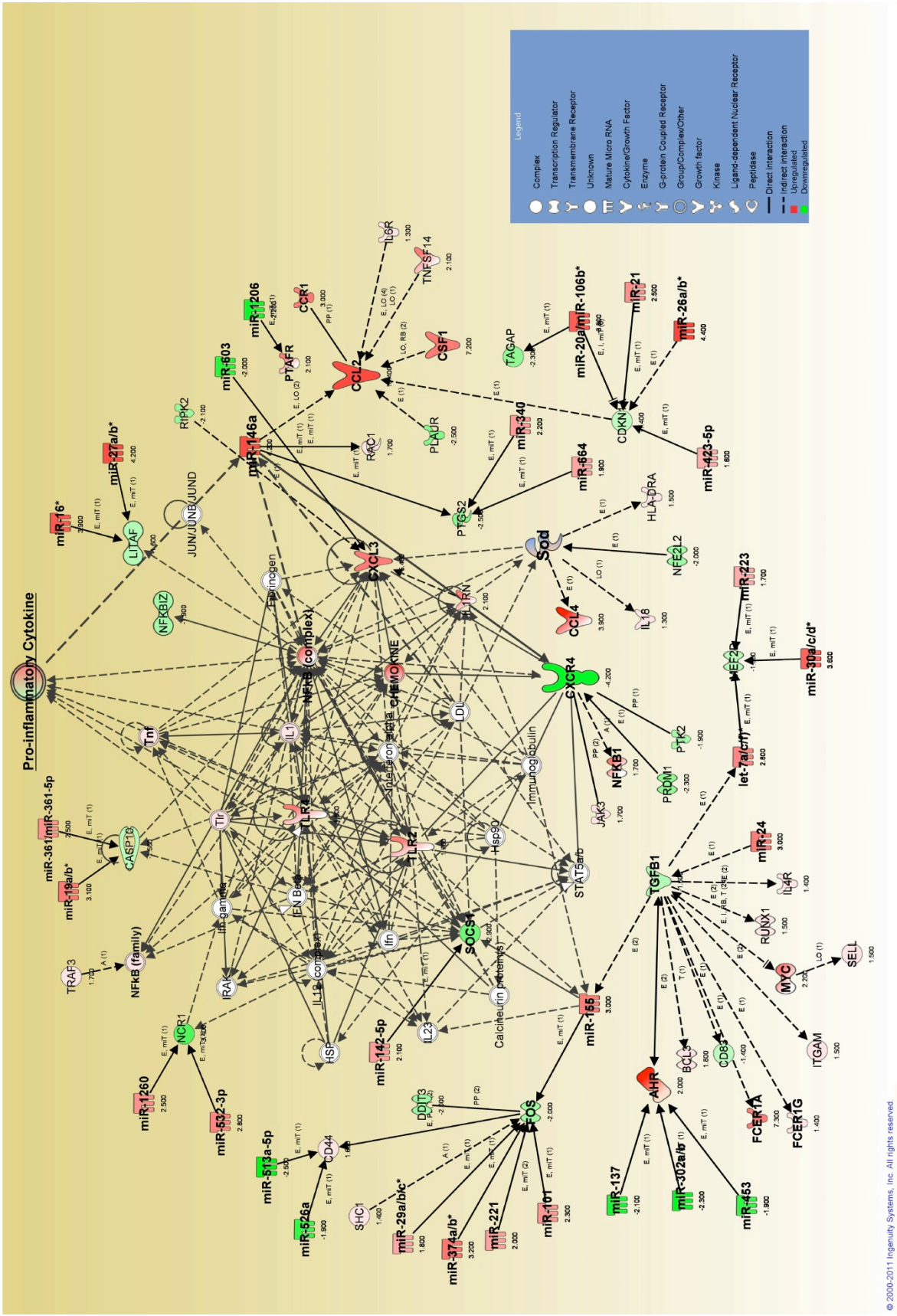

Supplemental Figure 12. microRNA-mRNA interactions in CD14+/CD16- blood monocytes in ALS. (A) MicroRNA target filter analysis (Ingenuity) based on significantly affected miRNAs (see Figure 15) and immune-related genes (see Figure 17) identified 32 miRNAs targeting 27 mRNAs in ALS subjects (see complete list of miRNA-mRNA interactions in Supplemental Table 6).

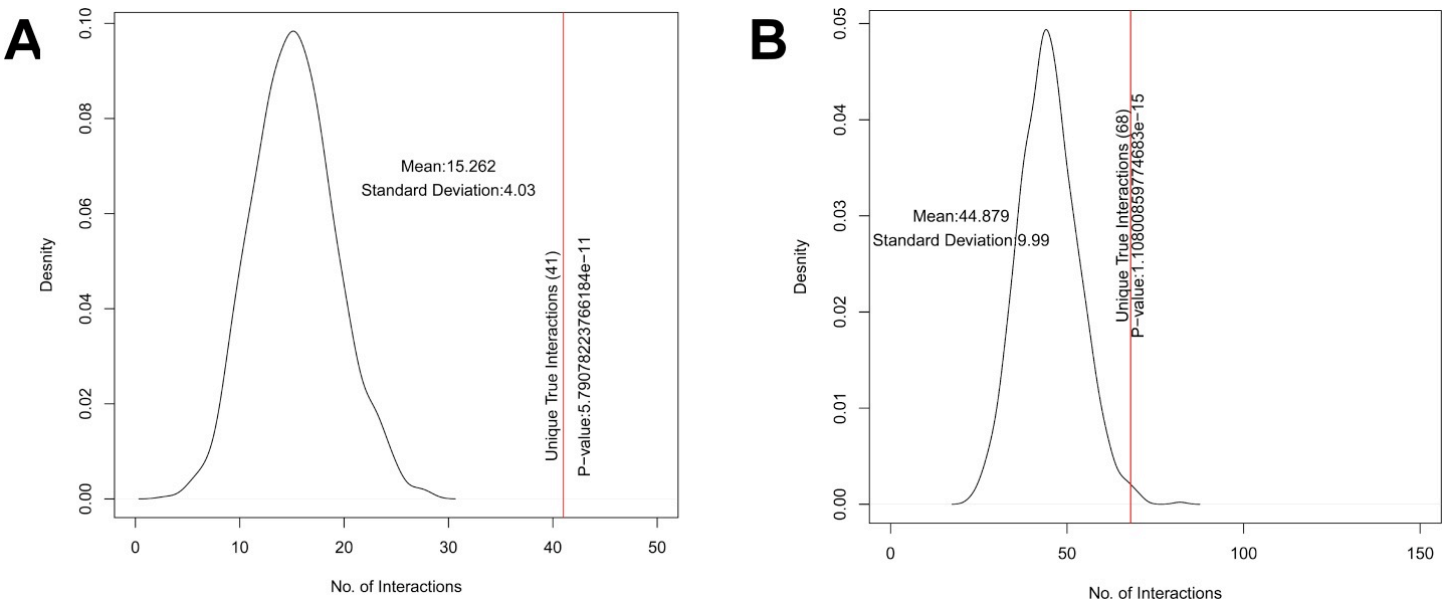

Supplemental Figure 13. Distribution of possible random interactions between 1000 of random non-regulated miRNA-mRNA pairs in comparison to observed putative miRNA-mRNA pairs in **(A)** 41 non-regulated highly expressed miRNAs and the 47 affected genes in splenic Ly6C^{Hi} monocytes in SOD1 mice (see Figure 4) and **(B)** 64 non-regulated highly expressed miRNAs and the 59 affected genes in CD14+/CD16- peripheral blood monocytes in ALS subjects (see Figure 15) shown to be statistically significant (Targetscan 4.1; see statistical analysis in Supplemental Methods).

Supplemental Fig. 14. The key transcription factors and target genes in CD14+/CD16- blood monocytes in ALS

A

#	Network	Total nodes	Seed nodes	p-Value	zScore	gScore
1	SP1	45	44	3.6E-136	192.12	192.12
2	AP-1	40	39	1.5E-119	180.61	180.61
3	RelA (p65 NF-kB subunit)	39	38	2.8E-116	178.22	178.22
4	c-Rel (NF-kB subunit)	33	32	6.8E-97	163.14	163.14
5	STAT3	33	32	6.8E-97	163.14	163.14
6	ETS1	33	32	6.8E-97	163.14	163.14
7	NF-kB1 (p50)	31	31	3.2E-95	163.07	163.07
8	c-Jun	32	31	1.0E-93	160.49	160.49
9	CREB1	32	31	1.0E-93	160.49	160.49
10	c-Myc	30	30	5.0E-92	160.41	160.41
11	STAT1	31	30	1.5E-90	157.8	157.8
12	PU.1	31	30	1.5E-90	157.8	157.8
13	p53	31	30	1.5E-90	157.8	157.8
14	NF-kB	29	29	7.4E-89	157.71	157.71
15	EGR1	30	29	2.2E-87	155.06	155.06
16	GCR-alpha	29	28	3.1E-84	152.27	152.27
17	C/EBPbeta	29	28	3.1E-84	152.27	152.27
18	HIF1A	29	28	3.1E-84	152.27	152.27
19	YY1	28	27	4.3E-81	149.43	149.43
20	SP3	27	26	5.8E-78	146.53	146.53

B

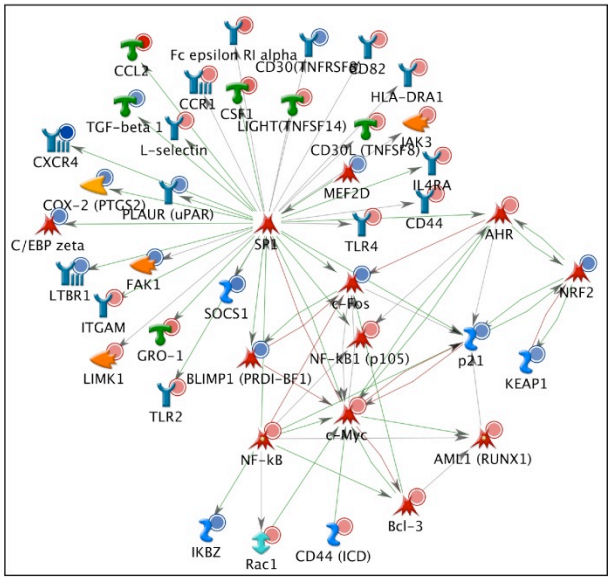

Supplemental Figure 14. **The key transcription factors and target genes in CD14+/CD16- blood monocytes in ALS.** **(A)** MetaCore™ (GeneGo) pathway analysis based on identified affected immune-related genes (see Figure 17) shows top 20 transcriptions factors and target genes. Note, 13 inflammation-related networks (highlighted in yellow) were identical to splenic Ly6C^{Hi} monocytes in SOD1 mice (see Table 3). **(B)** Specificity Protein 1 (SP-1) transcription factor and its targeted genes in CD14^{+}/CD16^{-} monocytes in ALS.

Supplemental Table 7. ALS Patients Donating Blood		
Characteristic	Disease Type	
	sALS	*fALS*
Number of patients	18	4
Disease duration (months) ± SD*	30.2 +/- 24.8	51.0 +/- 46.2
Age in Years ± SD	58.8 +/- 10.8	56.3 +/- 8.3
Percent Male	59%	75%
Mean ALSFRS-R	34.3	37.8
Site of Disease Onset		
Bulbar	18%	0%
Cervical	55%	0%
Lumbar	27%	100%
Unknown	0%	0%
** Disease onset taken as the first of the month for subjects who could identify the month, but not the day of disease onset.*		

Supplemental Table 8. ALS Patients Donating CSF			
Characteristic	Disease Type		
	sALS	*fALS*	*Healthy Controls*
Number of patients	10	5	10
Disease duration (months) +/-SD*	25.7 +/- 15.8	24.9 +/- 26.3	N/A
Age in Years +/- SD	52.1 +/- 14.6	38.8 +/- 12.0	56.9 +/- 14.8
Percent Male	90%	60%	80%
Site of Disease Onset:			
Bulbar	10%	0%	N/A
Cervical	30%	0%	N/A
Lumbar	50%	60%	N/A
Unknown	10%	40%	N/A
** Disease onset taken as the first of the month for subjects who could identify the month, but not the day of disease onset*			

Supplemental References

1. Leitner, M., Menzies, S., and Lutz, C. Prize4Life, Cambridge, MA and The Jackson Laboratory, Bar Harbor, ME. Working with ALS Mice. Guidelines for preclinical testing & colony management. .
2. Boillee, S., Yamanaka, K., Lobsiger, C.S., Copeland, N.G., Jenkins, N.A., Kassiotis, G., Kollias, G., and Cleveland, D.W. 2006. Onset and progression in inherited ALS determined by motor neurons and microglia. *Science* 312:1389-1392.
3. Scott, S., Kranz, J.E., Cole, J., Lincecum, J.M., Thompson, K., Kelly, N., Bostrom, A., Theodoss, J., Al-Nakhala, B.M., Vieira, F.G., et al. 2008. Design, power, and interpretation of studies in the standard murine model of ALS. *Amyotrophic lateral sclerosis : official publication of the World Federation of Neurology Research Group on Motor Neuron Diseases* 9:4-15.
4. Jung, S., Aliberti, J., Graemmel, P., Sunshine, M.J., Kreutzberg, G.W., Sher, A., and Littman, D.R. 2000. Analysis of fractalkine receptor CX(3)CR1 function by targeted deletion and green fluorescent protein reporter gene insertion. *Mol Cell Biol* 20:4106-4114.

5. Kettenmann, H., and Verkhratsky, A. 2008. Neuroglia: the 150 years after. *Trends in neurosciences* 31:653-659.
6. Cardona, A.E., Huang, D., Sasse, M.E., and Ransohoff, R.M. 2006. Isolation of murine microglial cells for RNA analysis or flow cytometry. *Nat Protoc* 1:1947-1951.
7. Asano, K., Nabeyama, A., Miyake, Y., Qiu, C.H., Kurita, A., Tomura, M., Kanagawa, O., Fujii, S., and Tanaka, M. 2011. CD169-Positive Macrophages Dominate Antitumor Immunity by Crosspresenting Dead Cell-Associated Antigens. *Immunity* 34:85-95.
8. Cedarbaum, J.M., Stambler, N., Malta, E., Fuller, C., Hilt, D., Thurmond, B., and Nakanishi, A. 1999. The ALSFRS-R: a revised ALS functional rating scale that incorporates assessments of respiratory function. BDNF ALS Study Group (Phase III). *Journal of the neurological sciences* 169:13-21.
9. Kasarskis, E.J., Dempsey-Hall, L., Thompson, M.M., Luu, L.C., Mendiondo, M., and Kryscio, R. 2005. Rating the severity of ALS by caregivers over the telephone using the ALSFRS-R. *Amyotrophic lateral sclerosis and other motor neuron disorders : official publication of the World Federation of Neurology, Research Group on Motor Neuron Diseases* 6:50-54.
10. Montes, J., Levy, G., Albert, S., Kaufmann, P., Buchsbaum, R., Gordon, P.H., and Mitsumoto, H. 2006. Development and evaluation of a self-administered version of the ALSFRS-R. *Neurology* 67:1294-1296.
11. Kurtzke, J.F. 1983. Rating neurologic impairment in multiple sclerosis: an expanded disability status scale (EDSS). *Neurology* 33:1444-1452.
12. Gabriely, G., Wurdinger, T., Kesari, S., Esau, C.C., Burchard, J., Linsley, P.S., and Krichevsky, A.M. 2008. MicroRNA 21 promotes glioma invasion by targeting matrix metalloproteinase regulators. *Molecular and cellular biology* 28:5369-5380.
13. Skog, J., Wurdinger, T., van Rijn, S., Meijer, D.H., Gainche, L., Sena-Esteves, M., Curry, W.T., Jr., Carter, B.S., Krichevsky, A.M., and Breakefield, X.O. 2008. Glioblastoma microvesicles transport RNA and proteins that promote tumour growth and provide diagnostic biomarkers. *Nature cell biology* 10:1470-1476.
14. Landgraf, P., Rusu, M., Sheridan, R., Sewer, A., Iovino, N., Aravin, A., Pfeffer, S., Rice, A., Kamphorst, A.O., Landthaler, M., et al. 2007. A mammalian microRNA expression atlas based on small RNA library sequencing. *Cell* 129:1401-1414.
15. Geiss, G.K., Bumgarner, R.E., Birditt, B., Dahl, T., Dowidar, N., Dunaway, D.L., Fell, H.P., Ferree, S., George, R.D., Grogan, T., et al. 2008. Direct multiplexed measurement of gene expression with color-coded probe pairs. *Nat Biotechnol* 26:317-325.
16. Guttman, M., Donaghey, J., Carey, B.W., Garber, M., Grenier, J.K., Munson, G., Young, G., Lucas, A.B., Ach, R., Bruhn, L., et al. 2011. lincRNAs act in the circuitry controlling pluripotency and differentiation. *Nature* 477:295-300.
17. Malkov, V.A., Serikawa, K.A., Balantac, N., Watters, J., Geiss, G., Mashadi-Hossein, A., and Fare, T. 2009. Multiplexed measurements of gene signatures in different analytes using the Nanostring nCounter Assay System. *BMC research notes* 2:80.
18. Kulkarni, M.M. 2011. Digital multiplexed gene expression analysis using the NanoString nCounter system. *Current protocols in molecular biology / edited by Frederick M. Ausubel ... [et al.]* Chapter 25:Unit25B 10.
19. Shipitsin, M., Campbell, L.L., Argani, P., Weremowicz, S., Bloushtain-Qimron, N., Yao, J., Nikolskaya, T., Serebryiskaya, T., Beroukhim, R., Hu, M., et al. 2007. Molecular definition of breast tumor heterogeneity. *Cancer cell* 11:259-273.